informs
http://pubsonline.informs.org/journal/trsc

TRANSPORTATION SCIENCE
Vol. 55, No. 2, March–April 2021, pp. 395–413
ISSN 0041-1655 (print), ISSN 1526-5447 (online)

The Robust Vehicle Routing Problem with Time Window Assignments

Maaike Hoogeboom,[a] Yossiri Adulyasak,[b] Wout Dullaert,[a] Patrick Jaillet[c]

[a] Department of Supply Chain Analytics, Vrije Universiteit Amsterdam, 1081 HV Amsterdam, Netherlands; [b] Group for Research in Decision Analysis and HEC Montréal, Montréal H3T 2A7, Québec, Canada; [c] Department of Electrical Engineering and Computer Science, Operations Research Center, Massachusetts Institute of Technology, Cambridge, Massachusetts 02139

Contact: m.hoogeboom@vu.nl, https://orcid.org/0000-0001-8512-0762 (MH); yossiri.adulyasak@hec.ca (YA); wout.dullaert@vu.nl (WD); jaillet@mit.edu (PJ)

Received: April 6, 2019
Revised: March 11, 2020
Accepted: June 25, 2020
Published Online in Articles in Advance: February 15, 2021

https://doi.org/10.1287/trsc.2020.1013

Abstract. In practice, there are several applications in which logistics service providers determine the service time windows at the customers, for example, in parcel delivery, retail, and repair services. These companies face uncertain travel times and service times that have to be taken into account when determining the time windows and routes prior to departure. The objective of the proposed robust vehicle routing problem with time window assignments (RVRP-TWA) is to simultaneously determine routes and time window assignments such that the expected travel time and the risk of violating the time windows are minimized. We assume that the travel time probability distributions are not completely known but that some statistics, such as the mean, minimum, and maximum, can be estimated. We extend the robust framework based on the requirements' violation index, which was originally developed for the case where the specific requirements (time windows) are given as inputs, to the case where they are also part of the decisions. The subproblem of finding the optimal time window assignment for the customers in a given route is shown to be convex, and the subgradients can be derived. The RVRP-TWA is solved by iteratively generating subgradient cuts from the subproblem that are added in a branch-and-cut fashion. Experiments address the performance of the proposed solution approach and examine the trade-off between expected travel time and risk of violating the time windows.

Funding: This research was enabled, in part, by support provided by Compute Canada and the Netherlands Organisation for Scientific Research [Grant 407-13-050]. This support is gratefully acknowledged.
Supplemental Material: The online appendix is available at https://doi.org/10.1287/trsc.2020.1013.

Keywords: vehicle routing • time window assignment • robust optimization • uncertain travel times

1. Introduction

In the vehicle routing problem (VRP) with time windows, service time windows are typically an input. In practice, however, there are many cases in which time windows are imposed by the service provider or are based on a mutual agreement or service-level agreement between the service provider and the customer. This is the case in attended home deliveries, for example, furniture delivery (Jabali et al. 2015), online grocery delivery (Campbell and Savelsbergh 2006), internet installation (Ulmer and Thomas 2019), and repair and maintenance services (Vareias, Repoussis, and Tarantilis 2017). When determining service time windows, there are often conflicting interests between customers and the service provider. On the one hand, customers typically prefer narrow time windows to limit the waiting time and to better plan their daily activities. The economic loss resulting from waiting for service at home was estimated at $38 billion in the United States in 2011 (Ellis 2011, Ulmer and Thomas 2019). On the other hand, service providers prefer wide time windows to have more routing flexibility and to lower the risk of violating the time window because of travel and service time uncertainties.

When planning an attended home delivery or service, customers can, in most cases, indicate an exogenous time window consisting of several hours during which they are available for service (Agatz et al. 2011, Klein et al. 2017). To improve the service and satisfaction of customers, service providers can then assign a smaller endogenous time window to each customer. The service providers, however, are faced with uncertain travel and service times that have to be taken into account when determining these endogenous time windows. This chapter considers the case in which a set of routes and endogenous time windows have to be generated before the travel times are known. The goal is to generate a robust routing plan and assign time windows to customers such that the risk of violating the time windows is minimized and the expected total travel time is below a certain threshold value.

The vehicle routing problem with time window assignments (VRP-TWA) and uncertain demand was introduced by Spliet and Gabor (2014). In this problem, time windows have to be assigned to customers before demand is known. When the demand is revealed, a vehicle routing schedule has to be generated that satisfies the assigned time windows. Spliet and Gabor (2014) assume that there is a set of demand scenarios that can occur and that time window assignments that minimize the average routing cost over these scenarios have to be found. Jabali et al. (2015) introduce a similar problem in which the demand is known but the travel times are uncertain. They assume that a disruption on an arc can occur with a certain probability and that the duration of this disruption is a discrete random variable with a known probability function. To reduce the number of scenarios, they assume that a disruption occurs on exactly one arc in a solution. The goal is to find an a priori routing plan and time window assignment that minimizes travel cost and time window violations. Vareias, Repoussis, and Tarantilis (2017) extend the work of Jabali et al. (2015) by allowing multiple arcs to be disrupted and by letting the duration of a disruption be a continuous random variable. They also propose a second model in which the travel time of each arc is a discrete random variable. Both Jabali et al. (2015) and Vareias, Repoussis, and Tarantilis (2017) solve a stochastic variant of the VRP-TWA in which the probability distributions are completely known, and in both papers a heuristic solution method is proposed. To handle cases where the probability distributions are hard to estimate, a robust optimization model can be used.

In this paper, the robust time window assignment vehicle routing problem (RVRP-TWA) is formulated in which the travel time probability functions are uncertain and only some descriptive statistics such as the mean, minimum, and maximum travel times are available. To measure the risk of violating the assigned time windows, the time window violation index proposed in Jaillet, Qi, and Sim (2016) is used. This measure incorporates the distributional statistics and is therefore less conservative than classical robust approaches where this information is ignored. Furthermore, both the frequency and magnitude of a violation are taken into account in this measure. The objective of the RVRP-TWA is to find routes and time window assignments that minimize the time window violation index. A solution method is proposed to solve the subproblem of finding the optimal time window assignment for each customer in a given route. By using a subgradient method implemented in a branch-and-cut framework, the RVRP-TWA is solved to optimality. The stochastic VRP-TWA (SVRP-TWA) is also discussed and used to illustrate the potential of the robust model. In the SVRP-TWA, the probability distributions of the travel times are assumed, violation is minimized, and the expected total travel time should be lower than a certain value. The SVRP-TWA is solved exactly using a branch-and-cut approach.

The main contributions of this research are as follows: (1) We are the first to propose a robust formulation for the VRP-TWA based on the risk measure proposed by Jaillet, Qi, and Sim (2016). (2) An efficient algorithm to optimize the time window assignments for a given set of routes is proposed. We show that this subproblem of finding the optimal time window assignment for a given route is convex and the subgradient can be derived, which allows for an efficient solution method. (3) A decomposition method is proposed to exactly solve the RVRP-TWA using the subgradient method in a branch-and-cut framework. (4) An exact solution method is proposed to solve the stochastic VRP-TWA. (5) Extensive computational experiments are performed to provide insights into working with limited data and to create a Pareto frontier of risk and expected total travel time.

The remainder of this chapter is organized as follows. In Section 2, the literature on robust vehicle routing and the VRP-TWA is reviewed. In Section 3, the RVRP-TWA and the feasible routing set are formally described. In Section 4, the robust solution framework is presented and the subproblem of finding the optimal time window assignment problem for a given route is solved. The branch-and-cut framework is presented in Section 5. The stochastic version of the VRP-TWA is proposed in Section 6. In Section 7, the computational results are discussed. Conclusions are presented in the final section.

2. Literature Review

The vehicle routing problem and many of its deterministic variants have been extensively studied; for literature reviews, see, for example, Golden, Raghavan, and Wasil (2008) and Toth and Vigo (2014). In practice, however, many parameters, such as customer demand, customer location, and travel times, are uncertain. Because larger amounts of data are becoming available, there has been an increase in the number of studies addressing the uncertain variants of the vehicle routing problem (Gendreau, Jabali, and Rei 2016). Generally speaking, there are two ways to deal with uncertainty: a stochastic approach in which the distribution of the uncertain parameter is known and a robust approach in which the probability distribution is hard to justify or estimate. The VRP with stochastic travel times was introduced by Laporte, Louveaux, and Mercure (1992) and extended by many others (Gendreau, Jabali, and Rei 2016). The extension including time windows is considered by, for example, Russell and

Urban (2008); Taş et al. (2013, 2014); Ehmke, Campbell, and Urban (2015); and Adulyasak and Jaillet (2016). In the robust VRP, uncertain parameters are characterized by uncertainty sets without information on the probability function; see, for example, Ordóñez (2010) for an overview. Recent studies present solution frameworks that incorporate some statistical information in the robust approach. For example, Lee, Lee, and Park (2012) and Agra et al. (2013) solve the VRP with time windows in which travel time uncertainty is defined using the budget of uncertainty as introduced by Bertsimas and Sim (2004). Jaillet, Qi, and Sim (2016) propose a method to solve the traveling salesman problem (TSP) with time windows in which the probability distributions of the travel times are unknown but some descriptive statistics, such as the mean, minimum, and maximum values, are known. They define a mathematical framework to solve this problem in an efficient and exact way. They propose a new measure to quantify the risk of violating a time window, taking into account both the frequency and the magnitude of the violations. The routing problem with the objective of minimizing the risk measure is solved using the Benders decomposition technique. The authors show that their robust solution approach is superior to existing models. Adulyasak and Jaillet (2016) extend this model to multiple vehicles and propose a stochastic model in which the probability distributions of the travel times are assumed to be known. Adulyasak and Jaillet (2016) are able to significantly reduce the computational time, compared with Jaillet, Qi, and Sim (2016), by using a branch-and-cut solution approach.

Zhang et al. (2019) propose a modification of the risk measure of Jaillet, Qi, and Sim (2016), to handle the TSP with hard time window as opposed to soft time windows. They assume that a vehicle can wait at no cost at the location of the customer if it arrives before the time window, but arriving after the time window should be avoided. Their proposed risk measure is less tight in measuring the probability of violation, but allows for a more tractable formulation for the VRP with hard time windows. Zhang et al. (2018) extend the measure of Zhang et al. (2019) by incorporating a parameter to customize the service level in terms of probabilistic guarantee of on-time delivery. They propose a data-driven framework using the Wasserstein ambiguity set, which is derived from empirical travel time data. In this chapter, we are dealing with soft time windows, where waiting at a customer before the start of the time window is impossible or costly.

In all the papers discussed above, the time windows are input, so they do not consider the time window assignment problem. Therefore, the frameworks of Jaillet, Qi, and Sim (2016) and Adulyasak and Jaillet (2016) cannot be directly applied to solve the proposed RVRP-TWA because the time windows are now decision variables instead of inputs. We will show that the new robust formulation is convex and that the subgradient can be derived. To measure the risk of violating the assigned time windows, the time window violation index proposed by Jaillet, Qi, and Sim (2016) will be used. A branch-and-cut approach, adapted from the original approach proposed in Adulyasak and Jaillet (2016), is developed to solve the RVRP-TWA.

The problem of assigning time windows to customers was recently introduced by Spliet and Gabor (2014) to solve a retail distribution problem. They propose the VRP-TWA with uncertain demand in which the deliveries to a store should always be made in the same fixed time window, whereas demand fluctuates per delivery. They assume that there is a set of demand scenarios that can occur and that the best time window assignments over these scenarios have to be found. In this VRP-TWA, the time windows have to be assigned before the demand is known, but the routes are made after the demand is revealed. As such, a different route per demand scenario has to be determined in the optimization process. The problem is solved using a branch-price-and-cut algorithm. Dalmeijer and Spliet (2018) improve the results of Spliet and Gabor (2014) by introducing a novel class of valid inequalities for this problem. The VRP-TWA with time-dependent travel times is introduced by Spliet, Dabia, and Van Woensel (2017). Instead of fixed travel times, they assume that the arcs have time dependent travel times to take the daily pattern of morning and evening rush hours into account.

Subramanyam and Gounaris (2017) show that the time window assignment problem with uncertain demand can be reduced to the consistent vehicle routing problem (ConVRP) with arrival time consistency requirements. In this problem, every customer must be visited multiple times in a certain period, and the difference between the earliest and latest arrival times at a customer must be lower than a certain constant. Using the branch-and-bound algorithm developed for the ConVRP, they are able to improve the results of Spliet and Gabor (2014). Their algorithm can also be used to consider uncertainty in travel times by constructing scenarios with different travel time perturbations.

Zhang et al. (2015) introduce the time window assignment problem for a maritime inventory routing problem. They look at a periodic setting in which the routes of the ships and the delivery time windows are decisions of the vendor. They take into account major disruptions of several days that result in several days' delay on a route or at a port. The problem is formulated as a two-stage stochastic mixed-integer program, and a two-phase solution approach is used in which, first, the routes are generated and, second, the time windows are allocated. In the routing phase, time buffers are inserted and the visits at a port are spread over the planning horizon. In the second phase, the time windows are assigned to every route by taking different disruption scenarios into account.

Jabali et al. (2015) introduce the vehicle routing problem with self-imposed time windows (VRP-SITW) in which delivery time windows at the customers are imposed by a logistic service provider. They assume that an arc will suffer a delay with a certain probability and that the duration of the delay is a discrete random variable with a known probability function. To reduce the number of scenarios, they assume that exactly one arc in a solution will suffer a delay. The goal is to construct an a priori routing plan and time window assignment such that the travel time, lateness, and overtime are minimized. A linear programming (LP) model is proposed to solve the time window assignment problem for a given route in which time buffers are allocated to customers to cope with possible delays. Estimates of this LP model are used in the proposed tabu search heuristic to solve the VRP-SITW. Vareias, Repoussis, and Tarantilis (2017) extend the work of Jabali et al. (2015) by allowing multiple arcs to be disrupted at the same time and by making the time window length a decision variable. They assume that the duration of a disruption at an arc is a continuous random variable with a known distribution. The model is discretized by partitioning the total density function into parts of equal probability. Vareias, Repoussis, and Tarantilis (2017) propose a second model in which the uncertainty follows from the stochastic travel times that are modeled as a set of scenarios. The distribution of the arrival time at a customer is given by the Cartesian product formed by all possible scenarios used by the arcs traveled to reach the customer. For both models, a mathematical model is proposed to solve the time window assignment problem for a given route. The objective of both models is to minimize the time window width, overtime, and earliness and lateness at a customer. The VRP-TWA is solved by an adaptive large neighborhood search algorithm in which, iteratively, the routing problem and the time window assignment problem are solved.

Both the papers of Jabali et al. (2015) and Vareias, Repoussis, and Tarantilis (2017) solve a variant of the stochastic VRP-TWA and present a heuristic solution method. We propose a model for the robust VRP-TWA in which the travel times of the arcs are not completely known. To the best of our knowledge, we are the first to tackle this problem. Furthermore, in our stochastic variant of the VRP-TWA, no scenarios or disruptions are assumed, but the probability distribution of the travel time of every arc is assumed to be known. An exact solution method to solve simultaneously the routing and time window assignment problems for both the robust and stochastic VRP-TWA is proposed.

3. Problem Description

The goal of the RVRP-TWA is to find an a priori routing solution and time window assignment that minimizes the risk of time window violations in terms of probability and magnitude of violations while the expected total travel time is kept below a certain threshold value, T.

To motivate the need for a robust solution method, an example of a VRP-based routing solution and a RVRP-TWA solution are presented in Figure 1. For the VRP-based solution, first, the routing problem is solved, and second, the optimal time windows are determined for the final routing solution. In the RVRP-TWA, the routing problem and time window assignments are solved simultaneously, as explained in Sections 4 and 5. For this instance, the risk of violating the time windows of the RVRP-TWA solution is 36% lower than in the VRP-based solution, although the travel time is only 4.3% higher.

In this section, the feasible routing set is described and the RVRP-TWA is formally proposed. Throughout this paper, boldface lowercase characters are used to indicate vectors, and a tilde ($\tilde{\cdot}$) is used to denote an uncertain parameter.

3.1. Routing Set

The RVRP-TWA is defined on a directed graph $G = (\mathcal{N}, \mathcal{A})$, with $\mathcal{N}$ the set of nodes and $\mathcal{A}$ the set of arcs. Let $\mathcal{K} = \{1, \ldots, K\}$ be the set of vehicles; then the set of nodes can be denoted by $\mathcal{N} = \{1, \ldots, n-1, n'_1, \ldots, n'_K, n\}$, with nodes 1 and n representing the depot and set $\mathcal{N}' = \{n'_1, n'_2, \ldots, n'_K\}$ representing the destination nodes of the vehicles. Similar to the notation used in Adulyasak and Jaillet (2016), the nodes in $\mathcal{N}'$

Figure 1. (Color online) The Routes of the VRP-Based and RVRP-TWA Solution Approaches for an Instance with 10 Customers

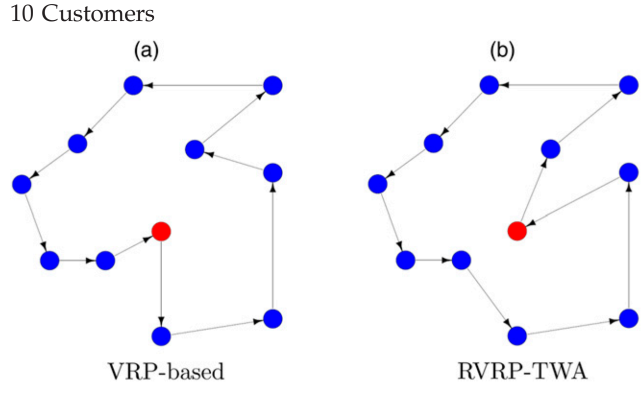

are copies of the depot node, and all incoming arcs are the same. The end depot node n is connected only to the vehicle destination nodes, that is, node n has K incoming arcs $(n'_k, n) \in \mathcal{A}$ with travel times equal to zero for all $k \in \mathcal{K}$. We assume that all nodes $\mathcal{N}$ must be visited except for the destination nodes $\mathcal{N}'$.

Let $\mathcal{N}_T \subset \mathcal{N}$ be the set of nodes with an exogenous time window, defined by $[e_i, l_i]$ for all $i \in \mathcal{N}_T$. To solve the time window assignment problem, an endogenous time window $[\tau_i, \tau_i + \epsilon_i] \subseteq [e_i, l_i]$ with start point τ_i and width ϵ_i has to be assigned to each node $i \in \mathcal{N}_T$. The start point of a time window τ_i is a decision variable, and ϵ_i is a constant. The depot nodes 1 and n do not have a time window restriction, but the vehicle destination nodes $\mathcal{N}'$ have fixed time windows, $[e_{n'_k}, l_{n'_k}] = [e_n, l_n]$ imposed. Hence, the endogenous time windows of the vehicle destination nodes $\mathcal{N}'$ are equal to the exogenous time windows, that is, $\tau_i = e_i$ and $\epsilon_i = l_i - e_i$ for all $i \in \mathcal{N}'$.

We assume that the endogenous time windows are soft, that is, if a vehicle arrives before or after the endogenous time window, the customer is immediately serviced. This is a reasonable assumption in our solution framework because (i) we enforce the expected arrival time at each customer to fall within the assigned time window (through Slater's condition described in Section 4.1), and (ii) the risk measure considered in this framework is an exponential function that takes into account both the frequency and magnitude of the time window violations, and thus routes that can potentially arrive much earlier or much later than the time window would be highly discouraged. Furthermore, we assume that the travel times are independent random variables. Let $\tilde{c}_a$ represent the uncertain travel time of arc $a \in \mathcal{A}$, with expected travel time c_a, minimum value $\underline{c}_a$, and maximum value $\bar{c}_a$. Jaillet, Qi, and Sim (2016) present a framework to deal with correlated travel times that can also be used in this setting, as explained in Section 8. Furthermore, we assume fixed service times s_i, $i \in \mathcal{N}$, which are added to the travel time $\tilde{c}_a$ with $a = (i, j)$. Note that the method described in this chapter can also be used when the service times are random variables. In this case, for all $i \in \mathcal{N} \backslash \mathcal{N}'$, a dummy node i' is created with only one incoming arc (i, i'), with travel time $\tilde{s}_i$.

To formulate the feasible routing set, the binary decision variables x_a and s_a^i are used. Variable x_a is one if arc a is used in the routing solution and zero otherwise, and s_a^i is equal to one if arc a is part of the route to node i. Variable z_i is equal to the number of times node $i \in \mathcal{N}$ is visited. For a given set of nodes $\mathcal{H} \subset \mathcal{N}$, let $\delta^-(\mathcal{H}) = \{(i,j) \in \mathcal{A} | i \in \mathcal{N} \backslash \mathcal{H}, j \in \mathcal{H}\}$ be the incoming arcs and

$\delta^+(\mathcal{H}) = \{(i,j) \in \mathcal{A} | i \in \mathcal{H}, j \in \mathcal{N} \backslash \mathcal{H}\}$ be the outgoing arcs. The capacity of every vehicle is Q, and let $r(\mathcal{H})$ be the minimum number of vehicles needed to serve the nodes in set $\mathcal{H}$. The routing set, $\mathcal{S}$, is defined by

$$\mathcal{S} = \{(\mathbf{s}, \mathbf{x}, \mathbf{z}) | (1) - (14)\}$$

$$1 \le z_i \le K, \qquad \forall i = \{1, n\}, \quad (1)$$

$$z_i = 1, \qquad \forall i \in \mathcal{N} \backslash (\mathcal{N}' \cup \{1, n\}), \quad (2)$$

$$z_i \le 1, \qquad \forall i \in \mathcal{N}', \quad (3)$$

$$\sum_{a \in \delta^-(i)} x_a = z_i, \qquad \forall i \in \mathcal{N} \backslash \{1\}, \quad (4)$$

$$\sum_{a \in \delta^+(i)} x_a = z_i, \qquad \forall i \in \mathcal{N} \backslash \{n\}, \quad (5)$$

$$\sum_{a \in \delta^+(1)} s_a^i = z_i, \qquad \forall i \in \mathcal{N}_T, \quad (6)$$

$$\sum_{a \in \delta^-(u)} s_a^i - \sum_{a \in \delta^+(u)} s_a^i = 0, \qquad \forall i \in \mathcal{N}_T, u \in \mathcal{N} \backslash \{1, i, n\}, \quad (7)$$

$$\sum_{a \in \delta^-(i)} s_a^i - \sum_{a \in \delta^+(i)} s_a^i = z_i, \qquad \forall i \in \mathcal{N}_T, \quad (8)$$

$$\sum_{a \in \mathcal{A}} c_a s_a^i \le T, \quad (9)$$

$$\sum_{a \in \delta^+(\mathcal{H})} x_a \ge r(\mathcal{H}), \qquad \forall \mathcal{H} \subset \mathcal{N}\{1, n\} |\mathcal{H}| \ge 2, \quad (10)$$

$$\sum_{a \in \mathcal{A}} c_a s_a^i \ge \sum_{a \in \mathcal{A}} c_a s_a^{i+1}, \qquad \forall i \in \mathcal{N}' \backslash \{n'_K\}, \quad (11)$$

$$0 \le s_a^i \le x_a, \qquad \forall i \in \mathcal{N}_T, \forall a \in \mathcal{A}, \quad (12)$$

$$z_i \in \mathbb{Z}^+, \qquad \forall i \in \mathcal{N}, \quad (13)$$

$$x_a \in \{0,1\}, \qquad \forall a \in \mathcal{A}. \quad (14)$$

Constraints (1) ensure that the number of vehicles used does not exceed the number of vehicles available. Constraints (2) state that all customers must be visited, and Constraints (3) ensure that the vehicle destination nodes can be visited at most once. Constraints (4) and (5) are the arc flow conservation constraints. Constraints (6)–(8) ensure the flow balance for every route to node $i \in \mathcal{N}_T$. Every route should start at the origin (Constraints (6)), and the flow balance should hold at the intermediate nodes (Constraints (7)) and the final node (Constraints (8)). Constraint (9) ensures that the expected total travel time does not exceed the threshold value T. Constraints (10) are the capacity and subtour elimination constraints. To avoid identical routing solutions with a different numbering of the vehicles, the symmetry breaking Constraints (11) are included. These ensure that the vehicles are numbered in order of decreasing expected travel time. Constraints (12) link the arc variables x_a and the route variables s_a^i; that is, arc a can be part of a route only if this arc is traversed in the solution. Note that $\mathbf{s} = (\mathbf{s}^i)_{i \in \mathcal{N}_T}$, with $\mathbf{s}^i$ the binary solution vector representing the route to node i.

The length of the assigned endogenous time window and the travel time threshold value T are input parameters. To find the lowest value of threshold T, the VRP with the objective to minimize the average total travel time can be solved before addressing the RVRP-TWA. Let T_0 be this minimum expected total travel time; then the travel time threshold value T is set to $T = \rho T_0$ with $\rho > 1$.

3.2. RVRP-TWA Problem Formulation

In the RVRP-TWA, it is assumed that the exact distribution of the uncertain travel times $\tilde{\mathbf{c}}$ is unknown but it belongs to a family of distributions $\mathbb{F}$. In addition, the travel times are independent random variables, and therefore the arrival time at node i is given by $\tilde{t}_i = \tilde{\mathbf{c}}\mathbf{s}^{\mathbf{i}}$. To obtain a robust solution and to capture the risk of violating the endogenous time windows, the exponential disutility function introduced in Jaillet, Qi, and Sim (2016) will be used. Let $C_{\alpha_i}(\tilde{t}_i)$ be the deterministic value representing the worst-case certainty equivalent of random arrival time $\tilde{t}_i$ at node i under risk tolerance parameter α_i. The term $C_{\alpha_i}(\tilde{t}_i)$ is defined as

$$C_{\alpha_i}(\tilde{t}_i) = \begin{cases} \sup_{\mathbb{P}\in\mathbb{F}} \alpha_i \ln \mathbb{E}_{\mathbb{P}}\left(\exp\left(\frac{\tilde{t}_i}{\alpha_i}\right)\right) & \text{if } \alpha_i > 0, \\ \lim_{\beta\downarrow 0} C_\beta(\tilde{t}_i) & \text{if } \alpha_i = 0. \end{cases}$$

This function has some interesting properties that will be used in our solution method. In particular, Jaillet, Qi, and Sim (2016) show that $C_{\alpha_i}(\tilde{t}_i)$ is jointly convex in $(\alpha_i, \tilde{t}_i)$. The risk of violating the endogenous time window $[\tau_i, \tau_i + \epsilon_i]$ at node i is measured by the time window violation index defined by

$$\rho_{\tau_i} = \inf\{\alpha_i + \eta_i | C_{\alpha_i}(\tilde{t}_i) \le \tau_i + \epsilon_i, C_{\eta_i}(-\tilde{t}_i) \le -\tau_i\}.$$

This is the smallest risk tolerance such that the certainty equivalent of the arrival time does not exceed the lower and upper bounds of the endogenous time window. Note that $\rho_{\tau_i} = 0$ when the arrival time is guaranteed to meet the time window $[\tau_i, \tau_i + \epsilon_i]$ because α and η are both equal to zero. Furthermore, the time window violation index takes both the probability and the magnitude of the violation into account. More properties and details of the time window violation index are discussed in Online Appendix A.

The objective of the RVRP-TWA is to find the routing solution $\mathbf{s} \in \mathcal{S}$ and endogenous time windows $\boldsymbol{\tau}$ with the lowest time window violation index. Hence, the optimal route and time window assignments can be found by solving the following optimization problem:

$$\inf \sum_{i\in\mathcal{N}_T} \alpha_i + \eta_i, \tag{15}$$

$$\text{s.t. } C_{\alpha_i}(\tilde{\mathbf{c}}\mathbf{s}^{\mathbf{i}}) \le \tau_i + \epsilon_i, \qquad \forall i \in \mathcal{N}_T, \tag{16}$$

$$C_{\eta_i}(-\tilde{\mathbf{c}}\mathbf{s}^{\mathbf{i}}) \le -\tau_i, \qquad \forall i \in \mathcal{N}_T, \tag{17}$$

$$e_i \le \tau_i \le l_i - \epsilon_i, \qquad \forall i \in \mathcal{N}_T, \tag{18}$$

$$\alpha_i, \eta_i \ge 0, \qquad \forall i \in \mathcal{N}_T, \tag{19}$$

$$\mathbf{s} \in \mathcal{S}. \tag{20}$$

The objective function (15) is to minimize the risk parameters. Constraints (16) and (17) ensure that the certainty equivalent of the arrival time does not exceed the bounds of the endogenous time window. The decision variables are presented in Constraints (18)–(20), in which Constraints (18) ensure that the endogenous time windows are included in the exogenous time windows.

4. Solution Framework

Solving problem (15)–(20) is challenging because function C_{α_i} is nonlinear in α_i and the entire formulation with the routing set $\mathcal{S}$ is a mixed-integer nonlinear program. Therefore, we apply a decomposition technique to solve this problem. First, the subproblem of minimizing the time window violation index for a given routing solution $\mathbf{s} \in \mathcal{S}$ is investigated. If $\bar{\mathbf{c}}\mathbf{s}^i - \underline{\mathbf{c}}\mathbf{s}^i < \epsilon_i$, then α_i and η_i are both zero. Otherwise, the subproblem with objective value $f(\mathbf{s})$ is given by

$$f(\mathbf{s}) = \inf \sum_{i\in\mathcal{N}_T} \alpha_i + \eta_i, \tag{21}$$

$$\text{s.t. } C_{\alpha_i}(\tilde{\mathbf{c}}\mathbf{s}^{\mathbf{i}}) \le \tau_i + \epsilon_i, \qquad \forall i \in \mathcal{N}_T, \tag{22}$$

$$C_{\eta_i}(-\tilde{\mathbf{c}}\mathbf{s}^{\mathbf{i}}) \le -\tau_i, \qquad \forall i \in \mathcal{N}_T, \tag{23}$$

$$\max\{e_i, \underline{\mathbf{c}}\mathbf{s}^i\} \le \tau_i \le \min\{l_i, \bar{\mathbf{c}}\mathbf{s}^i\} - \epsilon_i, \qquad \forall i \in \mathcal{N}_T, \tag{24}$$

$$\alpha_i, \eta_i \ge 0, \qquad \forall i \in \mathcal{N}_T. \tag{25}$$

Constraints (24) ensure that the start time of the endogenous time window is not lower than the lowest possible arrival time, $\underline{\mathbf{c}}\mathbf{s}^i$, and the end time of the endogenous time window is not higher than the latest possible arrival time, $\bar{\mathbf{c}}\mathbf{s}^i$. Furthermore, the endogenous time windows are included in the exogenous time windows. Because C_{α_i} is convex in α_i, problem (21)–(25) can be decomposed into $|\mathcal{N}_T|$ convex problems, each with three variables, α_i, η_i, and τ_i. Therefore, as stated in Proposition 1, $f(\mathbf{s})$ is a convex problem, and the proof can be found in Online Appendix B.

Proposition 1. *$f(\mathbf{s})$ is convex in* $\mathbf{s}$.

Proposition 1 allows us to derive subgradient cuts from the solution of $f(s)$. In the next section, we focus on deriving the subgradient of $f(\mathbf{s})$ using the Lagrange function, and we show that Benders decomposition can be used to solve the RVRP-TWA.

4.1. Derivation of the Subgradient of $f(\mathbf{s})$

To guarantee feasibility of the problem, ϵ_i and the exogenous time window boundaries e_i and l_i, for all $i \in \mathcal{N}_T$, should be defined such that there exists a solution $\mathbf{s}$ for which the following conditions hold:

$$\begin{aligned}
&\lim_{\alpha_i\to\infty} C_{\alpha_i}(\tilde{\mathbf{c}}\mathbf{s}^i) = \sup_{\mathbb{P}\in\mathbb{F}} \mathbb{E}_{\mathbb{P}}(\tilde{\mathbf{c}}\mathbf{s}^i) \le l_i, && \forall i \in \mathcal{N}_T,\\
&\lim_{\eta_i\to\infty} C_{\eta_i}(-\tilde{\mathbf{c}}\mathbf{s}^i) = \sup_{\mathbb{P}\in\mathbb{F}} \mathbb{E}_{\mathbb{P}}(-\tilde{\mathbf{c}}\mathbf{s}^i) \le -e_i, && \forall i \in \mathcal{N}_T,\\
&\sup_{\mathbb{P}\in\mathbb{F}} (\mathbb{E}_{\mathbb{P}}(\tilde{\mathbf{c}}\mathbf{s}^i) + \mathbb{E}_{\mathbb{P}}(-\tilde{\mathbf{c}}\mathbf{s}^i)) < \epsilon_i, && \forall i \in \mathcal{N}_T.
\end{aligned}$$

The first two conditions guarantee that the two worst cases of the expected arrival time at node i (early arrival and late arrival) are within the assigned time window. The third condition guarantees that the deviation between the two worst cases of the expected arrival time must be bounded by the time window size. These conditions ensure that the routing solution satisfies the time windows in expectation, which is important in practice.

Hence, if these three conditions hold, then there exists a solution $\mathbf{s}$ and $\boldsymbol{\tau}$ for which the following hold:

$$\begin{aligned}
&\lim_{\alpha_i\to\infty} C_{\alpha_i}(\tilde{\mathbf{c}}\mathbf{s}^i) = \sup_{\mathbb{P}\in\mathbb{F}} \mathbb{E}_{\mathbb{P}}(\tilde{\mathbf{c}}\mathbf{s}^i) \le \tau_i + \epsilon_i, && \forall i \in \mathcal{N}_T,\\
&\lim_{\eta_i\to\infty} C_{\eta_i}(-\tilde{\mathbf{c}}\mathbf{s}^i) = \sup_{\mathbb{P}\in\mathbb{F}} \mathbb{E}_{\mathbb{P}}(-\tilde{\mathbf{c}}\mathbf{s}^i) \le -\tau_i, && \forall i \in \mathcal{N}_T,\\
&e_i \le \tau_i \le l_i - \epsilon_i, && \forall i \in \mathcal{N}_T.
\end{aligned}$$

Because C_{α_i} is monotonic decreasing in α_i, this implies that Slater's condition is satisfied, and therefore $f(\mathbf{s})$ is a classical convex problem. Strong duality implies that $f(\mathbf{s}) = \sup_{\lambda\ge 0} \inf_{\alpha,\eta,\tau\ge 0} L(\mathbf{s},\boldsymbol{\alpha},\boldsymbol{\eta},\boldsymbol{\tau},\boldsymbol{\lambda})$, with the Lagrange function given by

$$\begin{aligned}
&L(\mathbf{s},\boldsymbol{\alpha},\boldsymbol{\eta},\boldsymbol{\tau},\boldsymbol{\lambda})\\
&\quad = \sum_{i\in\mathcal{N}_T} \alpha_i + \sum_{i\in\mathcal{N}_T} \eta_i + \sum_{i\in\mathcal{N}_T} \bar{\lambda}(C_{\alpha_i}(\tilde{\mathbf{c}}\mathbf{s}^i) - \tau_i - \epsilon_i)\\
&\qquad + \sum_{i\in\mathcal{N}_T} \underline{\lambda}(C_{\eta_i}(-\tilde{\mathbf{c}}\mathbf{s}^i) + \tau_i)\\
&\qquad + \sum_{i\in\mathcal{N}_T} \lambda_{1i}(e_i - \tau_i) + \sum_{i\in\mathcal{N}_T} \lambda_{2i}(\tau_i - l_i + \epsilon_i)\\
&\qquad + \sum_{i\in\mathcal{N}_T} \lambda_{3i}(\underline{\mathbf{c}}\mathbf{s}^i - \tau_i) + \sum_{i\in\mathcal{N}_T} \lambda_{4i}(\tau_i - \bar{\mathbf{c}}\mathbf{s}^i + \epsilon_i).
\end{aligned}$$

Because L is linear in $\boldsymbol{\tau}$ and $C_{\alpha_i}(\tilde{\mathbf{c}}\mathbf{s}^i)$ is jointly convex in $(\alpha_i, \mathbf{s}^i)$ for all $i \in \mathcal{N}_T$, the function $L(\mathbf{s},\boldsymbol{\alpha},\boldsymbol{\eta},\boldsymbol{\tau},\boldsymbol{\lambda})$ is jointly convex in $(\mathbf{s},\boldsymbol{\alpha},\boldsymbol{\eta},\boldsymbol{\tau})$, given $\boldsymbol{\lambda} \ge \mathbf{0}$. Based on strong duality, we will show that the subgradient of function $f(\mathbf{s})$ is equal to the subgradient of function $L(\mathbf{s},\boldsymbol{\alpha},\boldsymbol{\eta},\boldsymbol{\tau},\boldsymbol{\lambda})$ with respect to $\mathbf{s}$:

$$\begin{aligned}
&f(\mathbf{y}) - f(\mathbf{s})\\
&\quad = \sup_{\lambda\ge 0} \inf_{\alpha,\eta,\tau\ge 0} L(\mathbf{y},\boldsymbol{\alpha},\boldsymbol{\eta},\boldsymbol{\tau},\boldsymbol{\lambda}) - \sup_{\lambda\ge 0} \inf_{\alpha,\eta,\tau\ge 0} L(\mathbf{s},\boldsymbol{\alpha},\boldsymbol{\eta},\boldsymbol{\tau},\boldsymbol{\lambda}) && (26)\\
&\quad \ge \inf_{\alpha,\eta,\tau\ge 0} L(\mathbf{y},\boldsymbol{\alpha},\boldsymbol{\eta},\boldsymbol{\tau},\boldsymbol{\lambda}^*) - \inf_{\alpha,\eta,\tau\ge 0} L(\mathbf{s},\boldsymbol{\alpha},\boldsymbol{\eta},\boldsymbol{\tau},\boldsymbol{\lambda}^*) && (27)\\
&\quad = L(\mathbf{y},\boldsymbol{\alpha}^y,\boldsymbol{\eta}^y,\boldsymbol{\tau}^y,\boldsymbol{\lambda}^*) - L(\mathbf{s},\boldsymbol{\alpha}^*,\boldsymbol{\eta}^*,\boldsymbol{\tau}^*,\boldsymbol{\lambda}^*) && (28)\\
&\quad \ge d_s^L(\mathbf{s},\boldsymbol{\alpha}^*,\boldsymbol{\eta}^*,\boldsymbol{\tau}^*,\boldsymbol{\lambda}^*)(\mathbf{y}-\mathbf{s}) + d_\alpha^L(\mathbf{s},\boldsymbol{\alpha}^*,\boldsymbol{\eta}^*,\boldsymbol{\tau}^*,\boldsymbol{\lambda}^*) \times (\boldsymbol{\alpha}^y - \boldsymbol{\alpha}^*) + \\
&\qquad d_\eta^L(\mathbf{s},\boldsymbol{\alpha}^*,\boldsymbol{\eta}^*,\boldsymbol{\tau}^*,\boldsymbol{\lambda}^*)(\boldsymbol{\eta}^y - \boldsymbol{\eta}^*) + d_\tau^L(\mathbf{s},\boldsymbol{\alpha}^*,\boldsymbol{\eta}^*,\boldsymbol{\tau}^*,\boldsymbol{\lambda}^*) \times (\boldsymbol{\tau}^y - \boldsymbol{\tau}^*) && (29)\\
&\quad = d_s^L(\mathbf{s},\boldsymbol{\alpha}^*,\boldsymbol{\eta}^*,\boldsymbol{\tau}^*,\boldsymbol{\lambda}^*)(\mathbf{y}-\mathbf{s}). && (30)
\end{aligned}$$

Note that $\boldsymbol{\lambda}^* = \operatorname{argsup}_{\lambda\ge 0}(\inf_{\alpha,\eta,\tau\ge 0} L(\mathbf{s},\boldsymbol{\alpha},\boldsymbol{\eta},\boldsymbol{\tau},\boldsymbol{\lambda}))$ in the first inequality (27), and let $(\boldsymbol{\alpha}^y,\boldsymbol{\eta}^y,\boldsymbol{\tau}^y) = \operatorname{arginf}_{\alpha,\eta,\tau\ge 0} L(\mathbf{y},\boldsymbol{\alpha},\boldsymbol{\eta},\boldsymbol{\tau},\boldsymbol{\lambda}^*)$. Let $Z(\mathbf{s}) = \{(\boldsymbol{\alpha}^0,\boldsymbol{\eta}^0,\boldsymbol{\tau}^0,\boldsymbol{\lambda}^0) : L(\boldsymbol{\alpha}^0,\boldsymbol{\eta}^0,\boldsymbol{\tau}^0,\boldsymbol{\lambda}^0) = \sup_{\lambda\ge 0}\inf_{\alpha,\eta,\tau\ge 0} L(\mathbf{s},\boldsymbol{\alpha},\boldsymbol{\eta},\boldsymbol{\tau},\boldsymbol{\lambda})\}$, $(\boldsymbol{\alpha}^*,\boldsymbol{\eta}^*,\boldsymbol{\tau}^*,\boldsymbol{\lambda}^*) \in Z(S)$, and $(d_s^L(\mathbf{s},\boldsymbol{\alpha}^*,\boldsymbol{\eta}^*,\boldsymbol{\tau}^*,\boldsymbol{\lambda}^*), d_\alpha^L(\mathbf{s},\boldsymbol{\alpha}^*,\boldsymbol{\eta}^*,\boldsymbol{\tau}^*,\boldsymbol{\lambda}^*), d_\eta^L(\mathbf{s},\boldsymbol{\alpha}^*,\boldsymbol{\eta}^*,\boldsymbol{\tau}^*,\boldsymbol{\lambda}^*), d_\tau^L(\mathbf{s},\boldsymbol{\alpha}^*,\boldsymbol{\eta}^*,\boldsymbol{\tau}^*,\boldsymbol{\lambda}^*))$ be the subgradient vector of function $L(\mathbf{s},\boldsymbol{\alpha},\boldsymbol{\eta},\boldsymbol{\tau},\boldsymbol{\lambda}^*)$ at $(\mathbf{s},\boldsymbol{\alpha}^*,\boldsymbol{\eta}^*,\boldsymbol{\tau}^*)$. The second inequality follows from the fact that $L(\mathbf{s},\boldsymbol{\alpha},\boldsymbol{\eta},\boldsymbol{\tau},\boldsymbol{\lambda})$ is jointly convex in $(\mathbf{s},\boldsymbol{\alpha},\boldsymbol{\eta},\boldsymbol{\tau})$. Because $(\boldsymbol{\alpha}^*,\boldsymbol{\eta}^*,\boldsymbol{\tau}^*,\boldsymbol{\lambda}^*) \in Z(s)$, $d_\alpha^L(\mathbf{s},\boldsymbol{\alpha}^*,\boldsymbol{\eta}^*,\boldsymbol{\tau}^*,\boldsymbol{\lambda}^*) = 0$, $d_\eta^L(\mathbf{s},\boldsymbol{\alpha}^*,\boldsymbol{\eta}^*,\boldsymbol{\tau}^*,\boldsymbol{\lambda}^*) = 0$, and $d_\tau^L(\mathbf{s},\boldsymbol{\alpha}^*,\boldsymbol{\eta}^*,\boldsymbol{\tau}^*,\boldsymbol{\lambda}^*) = 0$, and this shows that $d_s^L(\mathbf{s},\boldsymbol{\alpha}^*,\boldsymbol{\eta}^*,\boldsymbol{\tau}^*,\boldsymbol{\lambda}^*)$ is equal to the subgradient of $f(\mathbf{s})$.

For $i \in \mathcal{N}_T$ with $\alpha_i^* = \eta_i^* = 0$, $\mathbf{s}^i$ is optimal; therefore, the following equation holds:

$$f(\mathbf{y}^i) - f(\mathbf{s}^i) = \alpha_i^y + \eta_i^y \ge d_{\mathbf{s}^i}^f(\mathbf{s})(\mathbf{y}^i - \mathbf{s}^i) \ge 0, \quad \forall \mathbf{y}^i \in \mathcal{S}^i.$$

This implies that $d_{s_a^i}^f(\mathbf{s}) = \mathbf{0}$ for all $a \in \mathcal{A}$.

Let $d_{s_a^i}^{c_1}(\alpha_i^*, \mathbf{s}^i)$ and $d_{s_a^i}^{c_2}(\eta_i^*, \mathbf{s}^i)$ be the subgradients of $C_{\alpha_i}(\tilde{\mathbf{c}}\mathbf{s}^i)$ and $C_{\eta_i}(-\tilde{\mathbf{c}}\mathbf{s}^i)$ with respect to s_a^i at point $(\alpha_i^*, \mathbf{s}^i)$ and $(\eta_i^*, \mathbf{s}^i)$, respectively. Deriving L along s_a^i, we obtain

$$d_{s_a^i}^L(\mathbf{s},\boldsymbol{\alpha}^*,\boldsymbol{\eta}^*,\boldsymbol{\tau}^*,\boldsymbol{\lambda}^*) = \bar{\lambda}^* d_{s_a^i}^{c_1}(\alpha_i^*, \mathbf{s}^i) + \underline{\lambda}^* d_{s_a^i}^{c_2}(\eta_i^*, \mathbf{s}^i) + \lambda_{3i}^* \underline{c}_a - \lambda_{4i}^* \bar{c}_a. \quad (31)$$

For $i \in \mathcal{N}_T$ with $\alpha_i^* \ne 0$ or $\eta_i^* \ne 0$, the Karush–Kuhn–Tucker (KKT) conditions are used to calculate the values of $\boldsymbol{\lambda}^*$ in Equation (31). Because strong duality holds, the KKT conditions are sufficient to find the optimal solution. Therefore, $\boldsymbol{\alpha}^*$, $\boldsymbol{\eta}^*$ and $\boldsymbol{\tau}^*$ are optimal if and only if the KKT conditions, presented in (32)–(43), hold:

$$d_{\alpha_i}^L(\mathbf{s},\boldsymbol{\alpha}^*,\boldsymbol{\eta}^*,\boldsymbol{\tau}^*,\boldsymbol{\lambda}^*) = 1 + \bar{\lambda}^* d_{\alpha_i}^{c_1}(\alpha_i^*, \mathbf{s}^i) = 0 \Rightarrow \bar{\lambda}^* = \frac{-1}{d_{\alpha_i}^{c_1}(\alpha_i^*, \mathbf{s}^i)}, \quad (32)$$

$$d_{\eta_i}^L(\mathbf{s},\boldsymbol{\alpha}^*,\boldsymbol{\eta}^*,\boldsymbol{\tau}^*,\boldsymbol{\lambda}^*) = 1 + \underline{\lambda}^* d_{\eta_i}^{c_2}(\eta_i^*, \mathbf{s}^i) = 0 \Rightarrow \underline{\lambda}^* = \frac{-1}{d_{\eta_i}^{c_2}(\eta_i^*, \mathbf{s}^i)}, \quad (33)$$

$$d_{\tau_i}^L(\mathbf{s},\boldsymbol{\alpha}^*,\boldsymbol{\eta}^*,\boldsymbol{\tau}^*,\boldsymbol{\lambda}^*) = \underline{\lambda}^* - \bar{\lambda}^* - \lambda_{1i}^* + \lambda_{2i}^* - \lambda_{3i}^* + \lambda_{4i}^* = 0, \quad (34)$$

$$\bar{\lambda}^*(C_{\alpha_i^*}(\tilde{\mathbf{c}}\mathbf{s}^i) - \tau_i^* - \epsilon_i) = 0, \quad (35)$$

$$\underline{\lambda}^*(C_{\eta_i^*}(-\tilde{\mathbf{c}}\mathbf{s}^i) + \tau_i^*) = 0, \quad (36)$$

$$\lambda_{1i}^*(e_i - \tau_i^*) = 0, \quad (37)$$

$$\lambda_{2i}^*(\tau_i^* - l_i + \epsilon_i) = 0, \quad (38)$$

$$\lambda_{3i}^*(\underline{\mathbf{c}}\mathbf{s}^i - \tau_i^*) = 0, \quad (39)$$

$$\lambda^*_{4i}(\tau^*_i - \bar{\mathbf{c}}\mathbf{s}^i + \epsilon_i) = 0, \tag{40}$$
$$C_{\alpha^*_i}(\tilde{\mathbf{c}}\mathbf{s}^i) \le \tau^*_i + \epsilon_i, \tag{41}$$
$$C_{\eta^*_i}(-\tilde{\mathbf{c}}\mathbf{s}^i) \ge -\tau^*_i, \tag{42}$$
$$\min\{e_i, \underline{\mathbf{c}}\mathbf{s}^i\} \le \tau^*_i \le \max\{l_i, \bar{\mathbf{c}}\mathbf{s}^i\} - \epsilon_i. \tag{43}$$

If $\alpha_i \neq 0$ or $\eta_i \neq 0$, then $C_{\alpha^*_i}(\tilde{\mathbf{c}}\mathbf{s}^i) = \tau^*_i + \epsilon_i$ and $C_{\eta^*_i}(-\tilde{\mathbf{c}}\mathbf{s}^i) = -\tau^*_i$, to keep α_i and η_i as low as possible. Otherwise, the objective can be improved by increasing the time window length. Using Equations (32) and (33), we get

$$\bar{\lambda}^* = \frac{-1}{d^{c_1}_{\alpha_i}(\alpha^*_i, \mathbf{s}^i)}$$

and

$$\underline{\lambda}^* = \frac{-1}{d^{c_2}_{\eta_i}(\eta^*_i, \mathbf{s}^i)}.$$

If τ^*_i is not bounded by the lower or upper bound, that is, if $\min\{e_i, \underline{\mathbf{c}}\mathbf{s}^i\} < \tau^*_i < \max\{l_i, \bar{\mathbf{c}}\mathbf{s}^i\} - \epsilon_i$, then $\lambda^*_{1i} = \lambda^*_{2i} = \lambda^*_{3i} = \lambda^*_{4i} = 0$ and $\alpha^*_i, \eta^*_i > 0$. Following Equation (34), this means that $\bar{\lambda}^* = \underline{\lambda}^*$, so $d^{c_1}_{\alpha_i}(\alpha^*_i, \mathbf{s}^i) = d^{c_2}_{\eta_i}(\eta^*_i, \mathbf{s}^i)$. If τ^*_i is bounded by $e_i, l_i - \epsilon_i, \underline{\mathbf{c}}\mathbf{s}^i$, or $\bar{\mathbf{c}}\mathbf{s}^i - \epsilon_i$, then the corresponding $\lambda^*_{1i}, \lambda^*_{2i}, \lambda^*_{3i}$, or λ^*_{4i} is nonzero. For example, if $\tau^*_i = \underline{\mathbf{c}}\mathbf{s}^i$, then $\lambda^*_{3i} = \underline{\lambda}^* - \bar{\lambda}^*$ to ensure that Equation (34) is equal to zero. Furthermore, a vehicle cannot arrive before $\underline{\mathbf{c}}\mathbf{s}^i$, so if $\tau_i = \underline{\mathbf{c}}\mathbf{s}^i$, then $\eta_i = 0$. Similarly, if $\tau_i = \bar{\mathbf{c}}\mathbf{s}^i - \epsilon_i$, then $\alpha_i = 0$. Therefore, the subgradient of $f(\mathbf{s})$ with respect to s^i_a can be calculated by

$$d^f_{s^i_a}(\mathbf{s}) = \begin{cases} \bar{\lambda}^* d^{c_1}_{s^i_a}(\alpha^*_i, \mathbf{s}^i) + \underline{\lambda}^* d^{c_2}_{s^i_a}(\eta^*_i, \mathbf{s}^i) & \alpha^*_i, \eta^*_i > 0, \\ \bar{\lambda}^* d^{c_1}_{s^i_a}(\alpha^*_i, \mathbf{s}^i) + \underline{\lambda}^* d^{c_2}_{s^i_a}(\eta^*_i, \mathbf{s}^i) & \\ \quad + \left(\underline{\lambda}^* - \bar{\lambda}^*\right)\underline{c}_a & \alpha^*_i > 0, \eta^*_i = 0, \\ \bar{\lambda}^* d^{c_1}_{s^i_a}(\alpha^*_i, \mathbf{s}^i) + \underline{\lambda}^* d^{c_2}_{s^i_a}(\eta^*_i, \mathbf{s}^i) & \\ \quad + \left(\underline{\lambda}^* - \bar{\lambda}^*\right)\bar{c}_a & \alpha^*_i = 0, \eta^*_i > 0, \\ 0 & \alpha^*_i = \eta^*_i = 0, \end{cases} \tag{44}$$

with

$$\bar{\lambda}^* = \frac{-1}{d^{c_1}_{\alpha_i}(\alpha^*_i, \mathbf{s}^i)}$$

and

$$\underline{\lambda}^* = \frac{-1}{d^{c_2}_{\eta_i}(\eta^*_i, \mathbf{s}^i)}.$$

The details of the computation of the subgradients $d^{c_1}_{s^i_a}(\alpha^*_i, \mathbf{s}^i)$, $d^{c_2}_{s^i_a}(\eta^*_i, \mathbf{s}^i)$, $d^{c_1}_{\alpha_i}(\alpha^*_i, \mathbf{s}^i)$, and $d^{c_2}_{\eta_i}(\eta^*_i, \mathbf{s}^i)$ are given in Online Appendix A. Using derivative (44), the RVRP-TWA model (15)–(20) can be reformulated as

$$\inf \quad w, \tag{45}$$
$$\text{s.t. } f(\mathbf{p}) + d^f_p(\mathbf{p})(\mathbf{s} - \mathbf{p}) \le w, \qquad \forall \mathbf{p} \in \mathcal{S}, \tag{46}$$
$$\sum_{a \in \mathcal{A}} \sup_{p \in \mathbb{F}} \mathbb{E}(\tilde{c}_a) s^i_a \le l_i, \qquad \forall i \in \mathcal{N}_T, \tag{47}$$
$$\sum_{a \in \mathcal{A}} \sup_{p \in \mathbb{F}} \mathbb{E}(-\tilde{c}_a) s^i_a \le e_i, \qquad \forall i \in \mathcal{N}_T, \tag{48}$$
$$\sum_{a \in \mathcal{A}} \left(\sup_{p \in \mathbb{F}} \mathbb{E}(\tilde{c}_a) - \sup_{p \in \mathbb{F}} \mathbb{E}(-\tilde{c}_a) \right) s^i_a \le \epsilon_i, \qquad \forall i \in \mathcal{N}_T, \tag{49}$$
$$\mathbf{s} \in \mathcal{S}. \tag{50}$$

Constraints (47)–(49) ensure that the solution is feasible. Problem (46)–(50) is solved using a branch-and-cut approach, described in Section 5. Because the routing set $\mathcal{S}$ is exponential in size, the subgradient cuts (46) are added in a branch-and-cut fashion.

4.2. Time Window Assignment for a Given Route

To solve problem (45)–(50), an efficient way to determine the optimal time window assignment for a routing solution is needed. Therefore, in this section, a method is proposed to efficiently determine the optimal values of $\boldsymbol{\alpha}, \boldsymbol{\eta}$, and $\boldsymbol{\tau}$ for a given routing solution $\mathbf{s}$. If $\bar{\mathbf{c}}\mathbf{s}^i - \underline{\mathbf{c}}\mathbf{s}^i \le \epsilon$, then $\tau_i = \underline{\mathbf{c}}\mathbf{s}^i$ is optimal because $\alpha_i = 0$ and $\eta_i = 0$. Otherwise, if $\bar{\mathbf{c}}\mathbf{s}^i - \underline{\mathbf{c}}\mathbf{s}^i > \epsilon$ and $\min\{e_i, \underline{\mathbf{c}}\mathbf{s}^i\} < \tau^*_i < \max\{l_i, \bar{\mathbf{c}}\mathbf{s}^i\} - \epsilon_i$, then we know from the KKT conditions that the optimal values α^*_i, η^*_i, and τ^*_i should satisfy the following three conditions:

1. $C_{\alpha^*_i}(\tilde{\mathbf{c}}\mathbf{s}^i) = \tau^*_i + \epsilon_i$,
2. $C_{\eta^*_i}(-\tilde{\mathbf{c}}\mathbf{s}^i) = -\tau^*_i$,
3. $d^{c_1}_{\alpha_i}(\alpha^*_i, \mathbf{s}^i) = d^{c_2}_{\eta_i}(\eta^*_i, \mathbf{s}^i)$.

The first and second conditions ensure that the values of α_i and η_i are as low as possible. The third condition implies that the objective cannot be improved, because both derivatives are equal; that is, decreasing α_i will increase η_i with the same value. This condition only holds if τ^*_i is not equal to a boundary point, that is, $\tau^*_i \neq e_i, \underline{\mathbf{c}}\mathbf{s}^i, l_i - \epsilon_i, \bar{\mathbf{c}}\mathbf{s}^i - \epsilon_i$. Because then $\lambda_k = 0$ for each k and $\bar{\lambda}^* = \underline{\lambda}^*$. In the proposed approach, initial checks are performed such that the boundary case is also covered.

The above three conditions will be used to efficiently solve problem (21)–(25), that is, to find the optimal values of α_i, η_i, and τ_i for route $\mathbf{s}^i$. Figure 2 illustrates how the optimal value of τ_i can be found for a simple example in which the route to customer i consists of a single arc $a = (0, i)$. Let $\tilde{c}_a$ be the travel time of this arc, with $\mathbb{F} = \{\mathbb{E}_{\mathbb{P}}(\tilde{c}_a) = 10, \mathbb{P}(\tilde{c}_a \in [7, 15]) = 1\}$. Note that the arrival time at customer i is $\tilde{t}_i = \tilde{c}_a$, because the route consists only of arc a. In the left graph, examples of the functions $C_{\alpha_i}(\tilde{t}_i)$ and $-C_{\eta_i}(-\tilde{t}_i)$ are given. In the right graph, the derivatives of $C_{\alpha_i}(\tilde{t}_i)$ and $C_{\eta_i}(-\tilde{t}_i)$ with respect to α_i and η_i are shown for different values of τ_i. When shifting graph $d^{c_1}_{\alpha_i}$ by ϵ_i units to the left, the crosspoint of this shifted graph with graph $d^{c_2}_{\eta_i}$ represents the optimal value of τ_i; that is, all three conditions hold at this crosspoint. The optimal values corresponding to Figure 2 are $\tau^*_i = 8.5$, $\alpha^*_i = 5.2$, and $\eta^*_i = 3.7$ given that $\epsilon_i = 3$.

Figure 2. (Color online) (Left) Examples of $C_{\alpha_i}(\tilde{t}_i)$ and $-C_{\eta_i}(-\tilde{t}_i)$ and (Right) the Derivatives of These Functions with Respect to α_i and η_i, Respectively

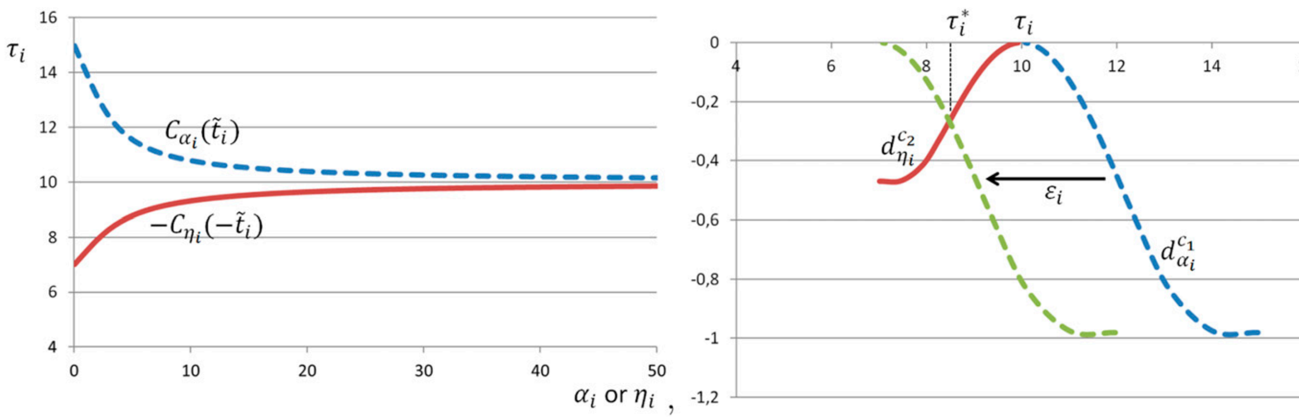

A variant of the binsearch algorithm is used to quickly determine this crosspoint. Instead of performing the binary search (binsearch) algorithm on only one variable, it is performed on both τ_i and the derivative value d^c. The lower and upper bounds of the derivative are initialized by $d_{lb} = -\infty$ and $d_{ub} = 0$, respectively. At every iteration, the variable with the smallest remaining solution space is chosen, and the midpoint of this solution space is selected as target value. Before starting the search, checks are carried out to see whether a crosspoint exists between $\tau_{lb} = \max\{e_i, \underline{\mathbf{cs}}^i\}$ and $\tau_{ub} = \min\{l_i, \bar{\mathbf{cs}}^i\} - \epsilon_i$; otherwise, the optimal value of τ_i is equal to one of these boundary points and we are done. The pseudocode of this algorithm is given in Algorithm 1.

Algorithm 1 (Calculate the Optimal τ_i^*)

1: Initialize: $\tau_i = \mathbf{cs}^i - \epsilon_i/2$, $\tau_{lb} = \max\{e_i, \underline{\mathbf{cs}}^i\}$, $\tau_{ub} = \min\{l_i, \bar{\mathbf{cs}}^i\} - \epsilon_i$, $d_{lb} = 0$, and $d_{ub} = -\infty$
2: **if** no crosspoint inside τ_{lb} and τ_{ub} **then**
3: return $\tau_i^* = \tau_{lb}$ or $\tau_i^* = \tau_{ub}$
4: **end if**
5: Calculate α_i and η_i using binsearch, s.t. $C_{\alpha_i}(t_i) = \tau_i + \epsilon$ and $C_{\eta_i}(-t_i) = -\tau_i$
6: Calculate the corresponding derivative values $dC_\alpha = d^{c_1}_{\alpha_i}(\alpha_i, \mathbf{s}^i)$ and $dC_\eta = d^{c_2}_{\eta_i}(\eta_i, \mathbf{s}^i)$
7: *Update lower and upper bounds:*
8: **if** $dC_\alpha < dC_\eta$ **then**
9: $d_{lb} = \max\{d_{lb}, dC_\alpha\}$, $d_{ub} = \min\{d_{ub}, dC_\eta\}$, $\tau_{ub} = \tau_i$
10: **else**
11: $d_{lb} = \max\{d_{lb}, dC_\eta\}$, $d_{ub} = \min\{d_{ub}, dC_\alpha\}$, $\tau_{lb} = \tau_i$
12: **end if**
13: **while** $\tau_{ub} - \tau_{lb} > \varepsilon$ and $d_{ub} - d_{lb} > \varepsilon$ **do**
14: **if** $d_{ub} - d_{lb} < \tau_{ub} - \tau_{lb}$ **then**
15: $d = (d_{ub} - d_{lb})/2$
16: Calculate the α_i and η_i using binsearch, s.t. $d^{c_1}_{\alpha_i}(\alpha_i, \mathbf{s}^i) = d^{c_2}_{\eta_i}(\eta_i, \mathbf{s}^i) = d$
17: Calculate the corresponding τ_i values, s.t. $\tau_\alpha = C_{\alpha_i}(t_i) - \epsilon_i$ and $\tau_\eta = -C_{\eta_i}(-t_i)$
18: *Update lower and upper bounds:*
19: **if** $\tau_\eta < \tau_\alpha$ **then**
20: $\tau_{lb} = \max\{\tau_{lb}, \tau_\eta\}$, $\tau_{ub} = \min\{\tau_{ub}, \tau_\alpha\}$, $d_{lb} = d$
21: **else**
22: $\tau_{lb} = \max\{\tau_{lb}, \tau_\alpha\}$, $\tau_{ub} = \min\{\tau_{ub}, \tau_\eta\}$, $d_{ub} = d$
23: **end if**
24: **else**
25: $\tau_i = (\tau_{ub} - \tau_{lb})/2$
26: Calculate α_i and η_i using binsearch, s.t. $C_\alpha(t) = \tau_i + \epsilon$ and $C_\eta(-t) = -\tau_i$
27: Calculate the corresponding derivative values $dC_\alpha = d^{c_1}_{\alpha_i}(\alpha_i, \mathbf{s}^i)$ and
28: $dC_\eta = d^{c_2}_{\eta_i}(\eta_i, \mathbf{s}^i)$
29: Update lower and upper bounds as in Lines 8–12
30: **end if**
31: **end while**
32: return $\tau_i^* = (\tau_{lb} + \tau_{ub})/2$

5. Branch-and-Cut Algorithm

Problem (45)–(50) is solved using a branch-and-cut algorithm. The subtour elimination Constraints (10) and the subgradient cuts (46) are added during the branch-and-bound process. When a solution at a branch-and-bound node violates the subtour elimination constraint, the violated constraint is added, and the problem of the current node is resolved. This process continues until no more constraints are violated. To detect and generate the violated subtour elimination constraints, the separation procedure of Lysgaard, Letchford, and Eglese (2004) for the VRP is used. The subgradient cuts (46) are derived from feasible integer routing solutions. When a feasible solution is found in the branch-and-bound tree, the corresponding cut is generated and added to the problem.

The subgradient cuts (46) constrain the risk of an entire solution $\mathbf{p} \in \mathcal{S}$. To strengthen the lower bound, risk cuts for individual customers are added. Let $\mathcal{A}^i_{\mathbf{p}} = \{a \in \mathcal{A} | p^i_a = 1\}$ be the set of arcs that are part of the route to customer i, and let $w_i^{\mathbf{p}}$ be the time window violation index encountered at customer $i \in \mathcal{N}_T$ in solution $\mathbf{p} \in \mathcal{S}$. The total time window violation index w can be decomposed in $w = \sum_{i \in \mathcal{N}_T} w_i$, with w_i the index of customer i. Next to the subgradient cuts (46), the following cuts are added to model (45)–(50) for every feasible integer solution $\mathbf{p} \in \mathcal{S}$ found in the branch-and-bound tree:

$$w_i^{\mathbf{p}} + \sum_{a \in \mathcal{A}_{\mathbf{p}}^i} w_i^{\mathbf{p}} (s_a^i - p_a^i) \le w_i \quad \forall i \in \mathcal{N}_T, \qquad \forall \mathbf{p} \in \mathcal{S}. \quad (51)$$

The left-hand side of Constraint (51) is equal to $w_i^{\mathbf{p}}$ if the solution vector $\mathbf{s}^i$ is equal to or contains $\mathbf{p}^i$, that is, if $\mathcal{A}_{\mathbf{p}}^i \subseteq \mathcal{A}_{\mathbf{s}}^i$. Otherwise, the left-hand side is negative.

6. Stochastic VRP-TWA

The objective of the stochastic VRP-TWA is to minimize the expected time window violation while ensuring that the expected total travel time is below a certain threshold value, T. In the SVRP-TWA, the probability distributions of the travel times are assumed to be known. Let $\tilde{t}_i$ be the uncertain arrival time variable at node i. Suppose that for a given solution $\mathbf{s}$, the arrival time density function at node i is given by $f_{t_i}^{\mathbf{s}}$. Then, for time window assignment $\boldsymbol{\tau}$, the expected time window violation at node i is given by

$$\beta_{\mathbf{s}}^i(\tau_i) = \int_{-\infty}^{\tau_i} (\tau_i - x) f_{t_i}^{\mathbf{s}}(x) dx + \int_{\tau_i + \epsilon_i}^{\infty} (x - \tau_i - \epsilon_i) f_{t_i}^{\mathbf{s}}(x) dx.$$

The optimal time window assignment for node i in solution $\mathbf{s}$ can be found by solving $\beta_{\mathbf{s}}^i = \min_{\tau_i \in [e_i, l_i - \epsilon_i]} \beta_s^i(\tau_i)$, with $\beta_{\mathbf{s}}^i$ the minimum expected time window violation for routing solution $s \in \mathcal{S}$. The optimal value of τ_i can be found by solving

$$\frac{\partial}{\partial \tau_i}\left(\int_{-\infty}^{\tau_i} (\tau_i - x) f_{t_i}^{\mathbf{s}}(x) dx + \int_{\tau_i + \epsilon_i}^{\infty} (x - \tau_i - \epsilon_i) f_{t_i}^{\mathbf{s}}(x) dx \right) = 0 \quad (52)$$

$$\Rightarrow \int_{-\infty}^{\tau_i} f_{t_i}^{\mathbf{s}}(x) dx - \int_{\tau_i + \epsilon_i}^{\infty} f_{t_i}^{\mathbf{s}}(x) dx = 0 \quad (53)$$

$$\Rightarrow F_{t_i}^{\mathbf{s}}(\tau_i) = 1 - F_{t_i}^{\mathbf{s}}(\tau_i + \epsilon_i). \quad (54)$$

The Leibniz integral rule is used to obtain Equation (53), and $F_{t_i}^s$ is the cumulative distribution function. Because $f_{t_i}^{\mathbf{s}}$ is positive, the second derivative of β_i^s is positive, that is, $f_{t_i}^s(\tau_i) + f_{t_i}^s(\tau_i + \epsilon_i) \ge 0$. Therefore, the value τ_i^* resulting from solving Equation (54) is the global minimum. Hence, for the optimal value τ_i^*, the probability of arriving before the start of the time window (τ_i^*) is equal to the probability of arriving after the closing time of the time window ($\tau_i^* + \epsilon_i$).

In the SVRP-TWA, the goal is to find the routing solution $\mathbf{s} \in \mathcal{S}$ that minimizes $\sum_{i \in \mathcal{N}_T} \beta_{\mathbf{s}}^i$. Hence, the stochastic model is defined by $\min_{\mathbf{s} \in \mathcal{S}} \sum_{i \in \mathcal{N}_T} \beta_s^i$. Because it is computational intensive to calculate β_s^i for all $I \in \mathcal{N}_T$ for all solutions $\mathbf{s} \in \mathcal{S}$, the problem has been reformulated as follows:

$$\inf \sum_{i \in \mathcal{N}_T} v_i, \quad (55)$$

$$\text{s.t. } \beta_{\mathbf{p}}^i + \sum_{a \in \mathcal{A}_{\mathbf{p}}^i} \beta_{\mathbf{p}}^i (s_a^i - 1) \le v_i, \qquad \forall i \in \mathcal{N}_T, \forall \mathbf{p} \in \mathcal{S}, \quad (56)$$

$$v_i \ge 0, \qquad \forall i \in \mathcal{N}_T, \quad (57)$$

$$\mathbf{s} \in \mathcal{S}. \quad (58)$$

The left-hand side of constraint (56) takes the value $\beta_{\mathbf{p}}^i$ if the arcs that are part of solution $\mathbf{p}^i$ are also contained in solution $\mathbf{s}^i$, that is, if $\mathcal{A}_{\mathbf{p}}^i = \mathcal{A}_{\mathbf{s}}^i$; otherwise, it takes a negative value. Similar to the subgradient cuts (46), Constraints (56) are added in a branch-and-cut fashion.

Note that the time window violation index could also be used in the stochastic model. In this case, the supremum term would disappear, and the expected value in $\alpha_i \ln \mathbb{E}(\exp(\tilde{t}_i / \alpha_i))$ could be calculated by a sampling-based approach. However, in the stochastic setting, the distribution is known, and therefore, the expected time window violation can be calculated directly, and the time window violation index is not needed to measure the risk.

6.1. Sampling-Based Approach

For some commonly used travel time distributions, for example, independent normal or gamma distributed travel times (Taş et al. 2013; Ehmke, Campbell, and Urban 2015), the arrival time distribution is easy to calculate, and thus Equation (54) can be easily solved. However, in many cases, it will be difficult to calculate the exact arrival time distribution $f_{t_i}^{\mathbf{s}}$. A common approach to calculate $\beta_{\mathbf{s}}^i$ is to perform a Monte Carlo sampling approach in which a set of scenarios of the travel time vector $\tilde{\mathbf{c}}$ is generated. Let Ω be the set of scenarios, and let $t_i^1, \ldots, t_i^{|\Omega|}$ be the corresponding arrival times at node i for solution $\mathbf{s}$. It is assumed that τ_i is an integer, for example, representing minutes. The optimal value of τ_i can be determined by solving

$$\min_{\tau_i \in [e_i, l_i - \epsilon_i]} \tilde{\beta}_{\mathbf{s}}^i(\tau_i) = \min_{\tau_i \in [e_i, l_i - \epsilon_i]} \frac{1}{|\Omega|} \sum_{\omega \in \Omega} |\min\{t_i^\omega - \tau_i, \tau_i + \epsilon_i - t_i^\omega, 0\}|. \quad (59)$$

In this sampling approach, $\tilde{\beta}_{\mathbf{s}}^i(\tau_i)$ represents the average violation of time window $[\tau_i, \tau_i + \epsilon_i]$ at node $i \in \mathcal{N}_T$ in solution $\mathbf{s}$ and can be used in Constraint (56). Note that $|\min\{t_i^\omega - \tau_i, \tau_i + \epsilon_i - t_i^\omega, 0\}|$ is a piecewise linear convex function with respect to τ_i. Thus, $\tilde{\beta}_{\mathbf{s}}^i(\tau_i)$ is a piecewise linear convex function and, therefore, only one search direction, $\tilde{\beta}^i_{\mathbf{s}}(\tau^*_i+1)$ or $\tilde{\beta}^i_{\mathbf{s}}(\tau^*_i-1)$, can lead to an improvement of $\tilde{\beta}^i_{\mathbf{s}}(\tau^*_i)$. This is used in Algorithm 2 to determine the optimal value of τ_i, that is, to solve Equation (59).

Algorithm 2 (Determine Optimal Value τ^*_i)

```
Initialize: τ*_i = min{max{e_i, (1/|Ω|) Σ_{ω∈Ω} t^ω_i − ε_i/2}, l_i − ε_i}
if β̃^i_s(τ*_i + 1) < β̃^i_s(τ*_i) then
    while β̃^i_s(τ*_i + 1) < β̃^i_s(τ*_i) and τ*_i + 1 ≤ l_i − ε_i do
        τ*_i = τ*_i + 1
    end while
else
    while β̃^i_s(τ*_i − 1) < β̃^i_s(τ*_i) and τ*_i − 1 ≥ e_i do
        τ*_i = τ*_i − 1
    end while
end if
```

7. Results

Various computational experiments are performed to evaluate the performance of the proposed algorithms. All algorithms are implemented in C# under Windows 7 using CPLEX 12.8.0. The experiments are performed on a single core of a workstation with a 2.1 GHz Intel Core E5-2683 v4 processor and 128 GB of random access memory. The maximum running time is set to two hours. Unless stated otherwise, the following parameter settings are used. The time window length is set to 30 minutes for all customers, that is, $\epsilon_i = \hat{\epsilon} = 30$ for all $i \in \mathcal{N}_T$. The exogenous time window is set to nine hours for all nodes $i \in \mathcal{N}_T$. The average total travel time can increase with maximum 5% compared with the minimal expected total travel time T_0, that is, $\rho = 1.05$. Furthermore, we assume that a time window has to be assigned to all customers, that is, $\mathcal{N}_T = \mathcal{N} \backslash \{1, n\}$.

7.1. Instances

As shown by Jaillet, Qi, and Sim (2016), the computational time of their algorithm using the binary variables s^i_a is very sensitive to the number of arcs. Jaillet, Qi, and Sim (2016) and Adulyasak and Jaillet (2016) use instances with $3n$ arcs that were randomly selected. As a result, in many of their instances, there is only a single feasible routing solution with an expected total travel time below $1.1T_0$ (i.e., 10% above the optimal expected total travel time based on the VRP solution), which makes their instances not useful to examine the trade-off between the risk and expected total travel time of various routing solutions. Therefore, we generated new instances for the RVRP-TWA based on the Solomon (1987) instances, and an arc selection method is proposed to reduce the number of arcs.

7.1.1. RVRP-TWA Instance Generation. In the RVRP-TWA, the mean, minimum, and maximum travel times of each arc are known. To compare the results of the RVRP-TWA with the results of the SVRP-TWA, we based these characteristics on specific distributions. In particular, instances based on triangular and shifted gamma distributed travel times were generated, because these distributions are often assumed in the stochastic VRP (Taş et al. 2013; Adulyasak and Jaillet 2016; Vareias, Repoussis, and Tarantilis 2017). The first three instance sets (T1, T2, and T3) are made using the triangular distribution, characterized by a minimum value $\underline{c}_a$, a maximum value $\bar{c}_a$, and a mode m_a. Let u_a be the Euclidean distance of arc $a \in \mathcal{A}$; then the minimum value of the travel time of this arc is randomly drawn from the interval $\underline{c}_a \in [0.8u_a, 1.2u_a]$, and the maximum value is similarly drawn from $\bar{c}_a \in [1.25u_a, 2.5u_a]$. The T1 instances are symmetric with mode $m_a = \frac{\underline{c}_a+\bar{c}_a}{2}$, and the T2 and T3 instances are right skewed with $m_a = \underline{c}_a + \frac{\bar{c}_a-\underline{c}_a}{4}$ and $m_a = \underline{c}_a$, respectively. The mean travel time needed in the robust approach is calculated by $c_a = \frac{\underline{c}_a+\bar{c}_a+m_a}{3}$. Instance sets G1, G2, and G3 are based on the shifted gamma distribution, and they are characterized by the shape parameter α and the rate parameter λ. For every arc $a \in \mathcal{A}$, parameters α_a and λ_a are randomly drawn from the intervals in Table 1. Let $G(0.01)$ be the inverse cumulative gamma distribution with probability 0.01. The travel time distribution of arc a is equal to the gamma distribution shifted $u_a - G(0.01)$ to the right. Therefore, the characteristics of the travel time of arc a are given by $\underline{c}_a = u_a$, $\bar{c}_a = u_a - G(0.01) + G(0.99)$, and $c_a = \alpha_a\lambda_a$. Note that the α and λ values in Table 1 are generated such that the average difference between the maximum and minimum travel times of an arc is between 16.2 and 17.2 for G1, G2, and G3. For the triangular instances, the minimum and maximum values are the same for the three instance sets T1, T2, and T3.

Per instance set, six different instances were generated based on the Solomon (1987) instances. To ensure feasible solutions with finite time window violation index values, the exogenous time window of every customer and that of the depot (planning horizon) are each set to nine hours. Because the time windows are the only difference between the instances in a Solomon (1987) set, there is one instance per Solomon (1987) set, that is, c1, c2, r1, r2, rc1, and rc2. The service times of the customers are adjusted based on the modification in the planning horizon;

Table 1. Parameters of the Different Types of Gamma Instances

Instance	α	λ
G1	[5,20]	1
G2	[2,3]	[1.5, 3]
G3	1	[2,5.5]

Table 2. Average Results of the Triangular Instances

	T1							T2							T3						
N	nS	nV	Time	Risk	nC	Δrisk (%)	Δtt (%)	nS	nV	Time	Risk	nC	Δrisk (%)	Δtt (%)	nS	nV	Time	Risk	nC	Δrisk (%)	Δtt (%)
10	6	1.2	0	36	6	−13	3	6	1.2	1	55	13	−38	3	6	1.2	1	74	7	−25	3
15	6	1.5	8	37	15	−57	3	6	1.5	17	52	20	−40	3	6	1.5	6	68	14	−44	4
20	6	1.7	22	104	17	−21	3	6	1.7	79	81	32	−47	3	6	1.7	31	134	17	−34	4
25	6	2.3	1,001	73	46	−52	4	6	2.0	405	176	36	−40	3	6	2.0	491	86	76	−31	4
30	2	2.5	4,921	107	32	−49	4	4	2.5	3,993	131	77	−34	4	3	2.5	5,108	185	79	−49	4
35	0	2.8	7,200	128	64	−35	5	1	2.8	6,608	132	44	−28	4	1	2.8	6,171	99	68	−38	4

that is, if the planning horizon increases by factor x, then the service time increases by factor x as well. The vehicle capacity and the location and demand of the customers remain the same as in the original Solomon (1987) instances. If instances with N customers are considered, then the first N customers of the original 100 customers are taken into account.

7.1.2. Arc Selection Measures. Because using a complete graph in the solution method unnecessarily leads to high computation times, we must find a way to reduce the number of arcs while maintaining high-quality solutions. Because the risk of violating the assigned time windows is being minimized, it is unlikely that arcs with a wide travel time distribution are used in the optimal solution. Furthermore, the expected travel time cannot increase too much compared with the minimum expected travel time of the capacitated vehicle routing problem (CVRP). Therefore, arcs with a high mean travel time and wide distribution are unlikely to be used in the optimal solution. Let c_a be the mean travel time of arc a, and let $\Delta_a = \bar{c}_a - \underline{c}_a$ be the difference between the maximum and minimum values of the travel time of arc a. To reduce the number of arcs, an arc measure is used to rank the arcs. Let $a = (i, j)$ be an arc; then the measure is given by $c_a/\mathbb{E}_{b\in\delta^-(j)}c_b + \Delta_a/\mathbb{E}_{b\in\delta^-(j)}\Delta_b$. The mean travel time of arc (i, j) is divided by the average mean travel time of the incoming arcs of node j, to measure the performance of the arc relative to the other incoming arcs of node j. The same holds for the difference parameter Δ_a. To reduce the number of arcs, the best three incoming arcs and the best three outgoing arcs are selected for every node. The performance of this arc selection measure compared with other measures is tested in Online Appendix C. The new instances generated by this measure have, on average, $5.7N$ edges in total. The characteristics of the instances are given in Online Appendix D. The average mean arc length decreases from G1 to G3 and from T1 to T3. Furthermore, the average difference between the maximum and minimum travel times, denoted by Δ, fluctuates by less than 1% between G1, G2, and G3 and between T1, T2, and T3.

7.2. Performance of the Branch-and-Cut Algorithm

In this section, the performance of branch-and-cut algorithm for the RVRP-TWA is tested. The objective is to find the routing solution with the lowest time window violation index while the expected travel time is below a certain threshold value. This threshold value is set to $1.05T_0$, with T_0 the minimum expected travel time of the VRP. For the VRP-based solution, the time windows are assigned such that the time window violation index is minimized; that is, the method in Section 4.2 is used to determine τ_i for all $i \in \mathcal{N}_T$ in the final routing solution. Hence, it is a two-step procedure of routing first and TWA second.

The average results of the triangular and gamma instances are presented in Tables 2 and 3, respectively. The number of customers in each instance is denoted in the first column. The number of instances solved out of six instances is reported in column "nS." The average number of vehicle used is reported in the column "nV," and the average computational time in seconds is reported in the column "Time." The average upper bound of the time window violation index is presented in column "Risk," and the average

Table 3. Average Results of the Gamma Instances

	G1							G2							G3						
N	nS	nV	Time	Risk	nC	Δrisk (%)	Δtt (%)	nS	nV	Time	Risk	nC	Δrisk (%)	Δtt (%)	nS	nV	Time	Risk	nC	Δrisk (%)	Δtt (%)
10	6	1.2	3	133	37	−19	4	6	1.2	2	125	28	−19	4	6	1.2	2	95	17	−26	3
15	6	1.5	65	233	71	−24	4	6	1.5	35	222	64	−23	4	6	1.5	24	176	29	−28	4
20	6	2.0	1,970	363	162	−26	4	6	2.0	1,001	352	106	−21	5	6	1.8	197	289	40	−31	5
25	3	2.3	4,661	450	159	−20	4	4	2.3	4,842	394	189	−34	4	6	2.0	2,558	446	129	−26	3
30	0	2.8	7,200	539	109	−26	4	1	2.7	6,833	711	102	−20	5	1	2.7	6,246	373	84	−26	5

number of subgradient cuts added to the formulation is presented in the column "nC." In columns "Δrisk" and "Δtt," the relative difference of the violation index and the travel time compared with the VRP-based solution are given. The difference is computed by $(R - R_0)/R_0$, with R_0 denoting the violation index corresponding to the VRP-based solution and R the violation index of the RVRP-TWA solution. A similar calculation is performed for the difference in travel time. If an instance is not solved within two hours and the upper bound of time window violation index is equal to zero, then no feasible solution is found and this solution is not taken into account when calculating the average values. The detailed results per instance can be found in Online Appendix E.

For the triangular instances, the time window violation index of both the VRP-based and the RVRP-TWA solutions increase on average from T1 to T3. Hence, instances with skewed travel times have a higher risk, because the magnitude of the violations increases. The difference in risk value between the robust solution and the VRP-based solution is, on average, 39%, whereas the travel time increases by only 3.6% on average. In Figure 1, the routing solutions of the VRP and RVRP-TWA are presented for the T3-r2 instance with 10 customers. It should be noted that for different values of N, the time window violation index of instance c1 is already zero for the VRP-based solution. Therefore, in this case, the RVRP-TWA will not improve the risk value.

For the gamma instances, the time window violation index values of both the RVRP-TWA and the VRP-based solutions decrease from G1 to G3. This is because the standard deviation of the difference between the maximum and minimum travel time increases from G1 to G3, whereas the average difference stays the same (see Online Appendix D). Therefore, for the G3 instances, there are more arcs with low variability, which results in lower risk values. The computational time also decreases from G1 to G3. The average difference in risk value compared with the VRP-based solution is 25%, whereas the travel time increases by, on average, 4.2%. The solutions of the G3 instances result in the highest reduction in time window violation index compared with the VRP-based solutions.

For both the triangular and gamma instances, the Set 2 Solomon (1987) instances have a higher time window violation index than the Set 1 instances. This is due to the larger vehicle capacity and shorter service times of the Set 2 instances (see Section 7.1.1 for the description of these adjusted Solomon (1987) instances). As a result, fewer vehicles are used and more customers are included in a single route, resulting in more uncertainty than in the Set 1 instances. Furthermore, for instances with $N \leq 20$ customers, the Set 2 Solomon (1987) instances are easier to solve than the Set 1 instances, because the Set 2 instances need only a single vehicle. The branch-and-cut algorithm solves all triangular instances with 25 or fewer customers to optimality and all gamma instances with 20 or fewer customers. For the instances with 30 customers, the algorithm solves nine triangular instances but only two gamma instances. The triangular instances are easier to solve because the standard deviation of the mean travel time and the standard deviation of the difference between the maximum and minimum travel time are both much higher in the triangular instances than in the gamma instances (see Online Appendix D). If the standard deviation of the mean travel time is larger, many arcs cannot be used in the optimal solution because of the constraint on the total expected travel time, which makes the instances easier to solve. Furthermore, the high standard deviation of the difference between the maximum and minimum travel times indicates that there are arcs with very low variability, which results in a low risk value. Therefore, the time window violation indexes of the triangular instances are lower than those of the gamma instances.

Overall, the computational time of the branch-and-cut algorithm is higher when more cuts are generated. The number of cuts represents the number of feasible solutions found by the algorithm. The computational time of the branch-and-cut algorithm significantly increases when the number of customers increases. The computational times of instances with 20 customers are, on average, 69 and 419 times higher than those of the instances with 10 customers, for the triangular and gamma instances, respectively. Note that if an instance is not solved, the lower bound is relatively low.

7.3. Evaluation of the Optimal Time Window Assignment Method

In the proposed solution framework, a time window assignment method is used to minimize the time window violation index for a given route, as described in Section 4.2. In this section, the performance of this time window assignment method is compared with other time window assignments policies. As in Vareias, Repoussis, and Tarantilis (2017), three different policies for τ_i are evaluated: τ_i is selected symmetrically around the average arrival time, that is, $\tau_i = \mathbf{cs}^i - \epsilon_i/2$; τ_i is skewed left with respect to the average arrival time, that is, $\tau_i = \mathbf{cs}^i - \epsilon_i$; and τ_i is skewed right with respect to the average arrival time, $\tau_i = \mathbf{cs}^i$. In these policies, the value of τ_i is fixed given the average arrival time at customer i. These policies can also be used in our solution framework. The definition of $f(\mathbf{s})$ and the subgradient of $f(\mathbf{s})$ for these three policies are described in Online Appendix F.

Table 4. Average Results for the Different Time Window Assignment Policies

	Min				Sym				Left				Right			
Instance	Risk	tt	V	sdV	Risk	tt	V	sdV	Risk	tt	V	sdV	Risk	tt	V	sdV
T1	62.2	278.7	0.18	1.0	62.4	278.8	0.18	0.9	437.0	278.5	8.02	12.0	484.7	279.3	8.92	12.2
T2	91.1	266.3	0.66	2.3	91.2	266.2	0.66	2.3	557.0	267.0	9.89	15.3	709.0	266.6	12.69	16.9
T3	90.7	253.5	1.20	4.6	91.1	253.1	1.21	4.7	499.7	252.2	10.88	18.3	890.1	252.9	19.06	24.8
Average	81.4	266.2	0.68	2.6	81.6	266.0	0.68	2.6	497.9	265.9	9.59	15.2	694.6	266.3	13.56	18.0
G1	296.7	316.3	4.96	13.5	297.2	316.3	4.94	13.4	2,123.8	316.5	31.01	43.2	2,379.2	315.6	34.60	41.7
G2	239.9	275.7	4.80	13.9	240.7	275.7	4.71	13.7	1,525.2	274.7	25.65	38.3	2,015.0	275.2	33.66	37.7
G3	252.1	273.3	8.13	21.8	253.2	273.3	7.88	21.3	1,406.9	272.6	25.33	42.7	2,171.7	271.8	41.56	42.2
Average	262.9	288.4	5.96	16.4	263.7	288.4	5.84	16.1	1,685.3	287.9	27.33	41.4	2,188.6	287.5	36.60	40.5

The average results of the four time window assignment policies on the instances with 10, 15, 20, and 25 customers are presented in Table 4. The results of the algorithm with the minimum time window violation index policy, described in Section 4.2, are presented in column "Min." The results of the algorithm with τ_i determined by the symmetric, left-skewed, and right-skewed policies around the average arrival time are presented in the columns "Sym" "Left," and "Right," respectively. For every time window assignment policy, the average time window violation index and the expected travel time of the final routing solution are reported in columns "Risk" and "tt," respectively. The average time window violation as defined in Section 6 is calculated using a simulation with 100,000 scenarios. This average violation and the corresponding standard deviation are given in columns "V" and "sdV," respectively.

Our proposed policy and the symmetric policy perform significantly better than the skewed left and right policies. Because the travel time distributions are right skewed, the probability of arriving earlier than the mean value is higher; therefore, the left-skew policy performs better than the right-skew policy. Our proposed policy has the lowest time window violation index. However, according to the simulation results, the symmetric policy performs slightly better in terms of average violation than our proposed policy. This is because the total travel time distribution is a sum of the travel time distribution of all arcs, and by the law of large numbers, the total distribution is flatter and more symmetric around the mean value than the original travel time distributions. Because the aim of the robust approach is to seek a robust solution that minimizes the worst-case distributions (shown in the column "Risk"), the robust solution may not necessarily be the best in terms of the average violation under a given distribution. However, one can see that the differences in the expected violations between the robust solution (column "Min") and the symmetric case (column "Sym") are very small. It should be noted that the difference in the average violations of the minimum and symmetric policies increases when the travel time distributions are more skewed (from T1 to T3 and G1 to G3).

In reality, some arcs are less sensitive to disruptions than others. Therefore, the instances were adjusted by assuming that 50% of the arcs in the arc set have a uniform travel time of length two around the mean travel time. The new instances are denoted by a prime symbol. The results of the minimum and symmetric time window assignment policies on these new instances are presented in Table 5. Because of the reduction of the variability of the travel times, the average time window violation index and average time window violation are lower for these new instances. Table 5 shows that the proposed minimum policy performs better than the symmetric policy in terms of the violation index, average violation, and standard deviation. The difference in risk between these two policies increases when the travel time distributions are more skewed. The lower standard deviation indicates that the proposed solution is more robust than the symmetric method. Based on these experiments, we conjecture that the difference between the minimum and symmetric policies increases when less arcs are sensitive to disruptions.

7.4. Comparison with Other Models

In this section, the proposed RVRP-TWA is compared with the SVRP-TWA and the VRP-based approach. The VRP-based approach is a two-step process of

Table 5. Average Results for the Minimum and Symmetric Time Window Assignment Policies

	Min				Sym			
Instance	Risk	tt	V	sdV	Risk	tt	V	sdV
T1′	26.4	284.0	0.06	0.4	26.4	284.6	0.05	0.4
T2′	14.8	273.7	0.01	0.1	14.9	273.3	0.01	0.2
T3′	39.2	264.7	0.29	1.8	39.8	264.6	0.36	2.1
Average	26.8	274.1	0.12	0.8	27.0	274.2	0.14	0.9
G1′	101.7	334.5	1.27	4.7	102.1	334.7	1.31	4.7
G2′	60.6	295.8	0.72	3.9	61.3	295.8	0.75	4.2
G3′	50.0	299.9	0.85	6.0	51.1	299.8	0.98	6.6
Average	70.8	310.0	0.95	4.9	71.5	310.1	1.01	5.2

route first and TWA second; that is, first, the routes are determined by minimizing the expected travel time, and second, the time windows are assigned for the final routing solution. In the VRP-based approach the travel time uncertainty is ignored when constructing the route, and the time windows are assigned such that the time window violation index is minimized, that is, using the method described in Section 4.2. This model will be compared with the proposed RVRP-TWA that takes characteristics of the travel time distributions into account.

The proposed SVRP-TWA assumes that the travel time distributions are known and the expected time window violation is minimized. The proposed algorithm for the SVRP-TWA is described in Section 6, and the sampling method with 100,000 scenarios is used in this experiment. Even though the stochastic and robust VRP-TWA models are developed for different purposes in which different assumptions and objectives are taken into account, the computational comparisons in this section provide interesting insights between the two approaches on different aspects.

The solutions of the three models are tested in a simulation to calculate the average time window violation, that is, the average number of minutes that a vehicle arrives too early or too late at all customers in the solution. To evaluate the robustness of the solutions, two different travel time distributions with the same characteristics are used. The first distribution is the triangular (or gamma) distribution of the original instances described in Section 7.1. As the second distribution, a mixture of two triangular distribution is used (called the MT distribution) which has the same mean, minimum, and maximum values as the original instance. This MT distribution has two modes which are different from the mode of the original function. Online Appendix G describes how these MT distributions are generated from the original distributions. For the VRP-based and robust approaches, the final solution will be the same for both distributions. For the stochastic approach, the distribution does matter. Therefore, two different travel time distributions of the SVRP-TWA are tested: one in which the original distribution is assumed (Stoch-T or Stoch-G) and one in which the new MT distribution is assumed (Stoch-MT). When the same scenarios are used in the SVRP-TWA as in the simulation, the SVRP-TWA gives the optimal solution when minimizing the average time window violation. This is not the case when the distribution used in the optimization model of the SVRP-TWA is different from the distribution used in the simulation.

The average results for each model are reported in Tables 6 and 7 for the instances with 10, 15, 20, and 25 customers. The results of the instances that were solved by all models are reported. The distribution used in the simulation is reported in the first column, the number of instances solved by all models is reported in the second column, and the model is given in the third column. For each method, the average computational time in seconds and the average time window violation index are presented in the columns “Time” and “Risk,” respectively. The other columns present the results from the simulation, with columns “avTT” and “sdTT” showing the average and standard deviation of the total travel time, respectively. The average number of minutes that all vehicles in a solution are too early, too late, and in total outside the time windows are reported in the columns “lbV,” “ubV,” and “V,” respectively. The standard deviation of the total violation is reported in column “sdV,” and the maximum violation over all scenarios in column “maxV.” In the last two columns, the numbers of scenarios with no time window violations and five or more violations are reported.

Table 6. Results for the VRP-Based Approach, RVRP-TWA, and SVRP-TWA with the Same Distribution in the SVRP-TWA as in the Simulation

												#V($\times$1000)	
Dist.	Solved	Model	Time	Risk	avTT	sdTT	lbV	ubV	V	sdV	maxV	0	≥5
T	71/72	VRP	14	126.2	**254.5**	**16.3**	0.5	1.0	1.5	5.0	101.2	89.8	3.0
		Robust	138	**80.8**	263.4	16.5	0.2	0.5	0.7	2.6	64.8	93.4	**1.4**
		Stoch-T	198	85.5	263.1	16.5	0.2	0.4	**0.6**	**2.4**	**62.9**	**93.9**	**1.4**
T-MT	70/72	VRP	13	126.7	**254.3**	**16.7**	38.1	42.7	80.8	40.9	247.2	29.8	55.8
		Robust	115	**81.4**	263.1	16.9	27.5	30.6	58.1	**29.4**	**183.4**	35.2	47.4
		Stoch-MT	184	99.4	263.4	16.9	23.0	33.4	**56.4**	31.4	188.2	**35.8**	**47.2**
G	59/72	VRP	4	338.2	**278.5**	**17.4**	2.9	6.3	9.2	23.3	419.7	65.5	12.6
		Robust	374	**260.2**	289.8	17.6	1.7	4.3	6.0	16.7	328.7	**71.9**	8.8
		Stoch-G	242	267.8	289.8	17.6	2.0	3.6	**5.6**	**15.0**	**308.9**	71.5	**8.7**
G-MT	58/72	VRP	4	332.8	**274.7**	**18.0**	69.0	76.6	145.6	84.6	571.3	4.3	80.3
		Robust	351	**256.1**	285.8	18.2	52.5	59.7	112.2	**67.7**	**469.1**	**5.7**	**73.7**
		Stoch-MT	200	288.3	285.7	18.2	46.7	63.5	**110.2**	70.5	475.8	5.6	75.2

Note. The bold font indicates the best results of the three different models. Dist., Distribution.

Table 7. Results for the RVRP-TWA and SVRP-TWA with Different Distribution in the Stochastic Model and in the Simulation

Dist.	Solved	Model	Time	Risk	avTT	sdTT	lbV	ubV	V	sdV	maxV	#V(×1000) 0	≥5
T	70/72	Robust	115	**81.4**	**263.0**	16.5	0.2	0.5	**0.7**	**2.6**	**65.6**	**93.3**	**1.4**
		Stoch-MT	184	99.4	263.3	16.5	0.2	0.8	1.0	3.3	73.0	91.2	1.8
T-MT	71/72	Robust	138	**80.8**	263.4	**16.9**	27.2	30.4	**57.6**	**29.2**	**182.9**	**34.9**	**47.7**
		Stoch-T	198	85.5	**263.2**	17.0	30.7	29.1	59.8	30.1	183.1	32.4	49.2
G	58/72	Robust	351	**256.1**	**285.9**	17.5	1.7	4.3	**6.0**	**16.7**	**329.6**	**72.2**	**8.7**
		Stoch-MT	245	288.3	286.1	17.5	1.1	6.1	7.2	18.8	340.5	69.5	9.4
G-MT	59/72	Robust	374	**260.2**	**289.7**	18.3	52.0	59.2	**111.2**	67.6	471.5	5.8	**73.4**
		Stoch-G	242	267.8	**289.7**	18.3	58.9	53.8	112.7	**65.8**	**449.2**	**6.4**	74.7

Note. The bold font indicates the best results of the three different models. Dist., Distribution.

In Table 6, the distributions used in the stochastic model and in the simulation are the same. As expected, the average total travel time is lowest for the VRP-based approach, and the robust solution has the lowest time window violation index. The standard deviation of the total travel time is also lowest for the VRP-based approach. The travel time of the RVRP-TWA can increase by a maximum of 5% compared with the VRP-based solution; however, the results show that the increase in travel time is less than 4% on average. The average decrease in the time window violation index when using the RVRP-TWA instead of the VRP-based solution is 30%, and the decrease in the average violation is even higher (36%). The standard deviation and maximum violations are lower for the RVRP-TWA. Furthermore, for the solution of the RVRP-TWA, there are more scenarios without violations, and the number of scenarios with five violations or more is lower for the RVRP-TWA than for the VRP-based approach. Hence, for a relatively small increase in travel time (4%), the accuracy of being on time increases a lot when using the RVRP-TWA instead of the VRP-based approach.

The stochastic model gives the optimal solution when minimizing the average violation. The RVRP-TWA increases by, on average, 6% compared with the optimal SVRP-TWA. However, the numbers of scenarios without violations or with five violations or more are similar for the two models. Furthermore, for the MT distribution, the standard deviation of the violation and the maximum violation are lower for the robust model. The average and standard deviation of the travel time are almost the same for the robust and stochastic models. Thus, although the robust method has fewer data requirements than the stochastic variant, it performs very well.

In Table 7, the distribution assumed in the stochastic model and the distribution used in the simulation are different. Because the characteristic of both distributions are the same, the solutions of the VRP-based and the robust model stay the same as in Table 6. Therefore, the VRP-based results are excluded from this table. Table 7 compares the performance of the stochastic and robust approaches when no accurate estimate could be made on the actual travel time distributions. The results show that the robust model performs significantly better than the stochastic model. The average violation of the RVRP-TWA is, on average, 14% lower than that of the SVRP-TWA model, and the number of scenarios with five violations or more is lower for the RVRP-TWA. Furthermore, in most cases, the standard deviation and the maximum violation of the robust model are also lower than those of the stochastic model. Hence, the robust solution method is much less sensitive to distributional uncertainty than the stochastic solution approach.

Overall, the simulation with the MT distribution leads to higher violations and more violations per scenario. This is because the modes in the MT distribution are further away from the mean travel time. It should be noted that if the time window violation index decreases a lot, then the average time window violation decreases as well. If the differences in time window violation index are small, then a higher index value does not imply a higher average time

Table 8. Average Time Window Violation Index Values and Computational Times for Different Time Window Lengths

Inst.	N	Solved	$\hat{\epsilon}=15$ Time	Risk	$\hat{\epsilon}=30$ Time	Risk	$\hat{\epsilon}=45$ Time	Risk
T	10	18/18	0.7	156.4	0.6	54.8	0.5	24.2
	15	18/18	10.9	153.2	10.4	52.2	6.5	22.6
	20	18/18	57.1	277.2	44.2	106.6	34.6	53.3
	25	18/18	699.0	268.5	632.1	111.7	1,092.4	64.0
Average			191.9	213.8	171.8	81.3	283.5	41.0
G	10	18/18	2.1	271.8	2.3	117.9	2.3	64.7
	15	18/18	33.1	473.7	41.3	210.5	40.7	119.9
	20	15/18	167.3	777.9	182.7	360.0	186.7	215.9
	25	12	2,492.5	972.8	2,574.3	456.7	2,833.9	276.5
Average			524.6	583.5	546.3	266.5	596.5	156.8

Note. Inst., Instance.

Figure 3. (Color online) Pareto Frontier for Instance T2-r1 with 20 Customers

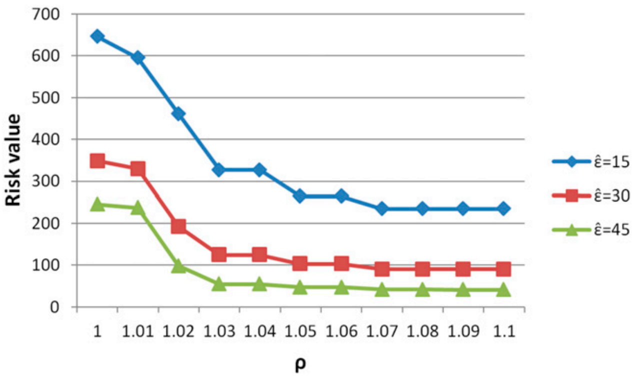

window violation. Thus, the time window violation index is a good measure for the average time window violation when the difference between solutions is not too small.

7.5. Pareto Frontier

In the RVRP-TWA, the time window violation index is minimized, and the expected travel time must be below ρT_0. Until now, it has been assumed that $\rho = 1.05$; hence, the expected travel time could increase by a maximum of 5% compared with the minimum expected travel time of the VRP. Furthermore, the time window length was set to $\epsilon_i = \hat{\epsilon} = 30$ $\forall i \in \mathcal{N}_T$, where $\hat{\epsilon}$ is a predefined window length. In this section, we will investigate the sensitivity of the proposed branch-and-cut algorithm to these two parameters and show the trade-off between travel time and the risk value.

In Table 8, the average time window violation index values and computational times are given for different values of $\hat{\epsilon}$ for the triangular and gamma instances. The second column represents the number of customers taken into account, and the number of instances solved is reported in column "Solved." An instance is taken into account only if it is solved for all $\hat{\epsilon}$ values. Trivially, the time window violation index decreases when the time window length increases. For the triangular instances, the time window violation index decreases by, on average, 62% from $\hat{\epsilon} = 15$ to $\hat{\epsilon} = 30$, and by 50% from $\hat{\epsilon} = 30$ to $\hat{\epsilon} = 45$. For the gamma instances, these decreases are 54% and 41%. Hence, the decrease in the time window violation index is not linear. The incremental decrease in the risk value declines when the number of customers increases. For instance T2-r1, the Pareto frontier for different time window lengths and travel time threshold values is presented in Figure 3. For this instance, it is shown that the risk gap between time window lengths of 15 and 30 minutes is much larger than the gap between 30 and 45 minutes. Because the travel time threshold is set to $\rho = 1.05$, the average travel time stays the same for all ϵ values.

The influence of the travel time threshold parameter ρ is presented in Table 9. When the threshold increases, the solution space of the feasible routing solutions increases, and therefore the computational time increases. On average, the computational time increases faster when more customers are taken into account in the instances. Because of this increase in solution space, the time window violation index decreases. This decrease in violation index is, on average, 14% from $\rho = 1$ to $\rho = 1.025$ and 16% from $\rho = 1.025$ to $\rho = 1.05$. For larger threshold values, this incremental decrease in the time window violation index declines. The example in Figure 3 illustrates the steep decrease in the time window violation index when ρ is increased from 1.01 to 1.03 and that this decrease tapers off when ρ increases. The frontier is S shaped because ρ should increase enough such that there exists a new routing solution with a lower violation index, and when the optimal routing solution is found, increasing ρ does not help anymore. In column "Δtt," the difference in the average travel time compared with the VRP-based solution ($\rho = 0$) is shown. When the average travel time threshold is set

Table 9. Average Time Window Violation Index Values and Computational Times for Different Threshold Values

			$\rho = 1$		$\rho = 1.025$			$\rho = 1.05$			$\rho = 1.075$			$\rho = 1.1$		
Inst.	N	Solved	Time	Risk	Time	Risk	Δtt (%)	Time	Risk	Δtt (%)	Time	Risk	Δtt (%)	Time	Risk	Δtt (%)
T	10	18/18	0	81	0	70	0.6	1	55	3.1	1	41	5.4	1	39	6.2
	15	18/18	2	92	3	71	1.4	9	52	3.6	22	49	4.8	42	48	6.4
	20	18/18	3	176	15	137	1.4	51	107	3.4	110	102	5.4	259	99	6.8
	25	12/18	7	150	50	133	1.6	238	128	3.3	567	126	5.1	1,695	125	6.8
Average			3	122	14	100	1.3	60	81	3.4	140	75	5.2	391	73	6.6
G	10	18/18	0	147	1	131	1.0	2	118	3.9	5	109	5.2	10	106	7.7
	15	18/18	1	275	8	235	1.8	40	210	4.1	171	193	6.3	643	184	8.7
	20	14/18	8	469	28	428	1.8	177	343	4.4	1,150	316	6.6	1,573	301	8.7
Average			3	283	11	251	1.6	65	214	4.2	385	198	6.1	675	189	8.4

Note. Inst., Instance.

to $\rho = 1.05$, an increase of 5% of the travel time is allowed. However, the travel time of the final solution increases by, on average, 3.4% for a triangle instance and by 4.2% for a gamma instance.

From a managerial point of view, the risk of violating a time window can be significantly reduced by allowing the travel time to increase by only 2.5%–5%. Furthermore, the time window length can be chosen corresponding to the preferred risk certainty.

8. Conclusions and Future Research

In the VRP-TWA, the time window assignment problem and the vehicle routing problem are combined. Recent papers proposed heuristic solution methods to solve the stochastic VRP-TWA in which the probability distributions of the travel times are known. We are the first to formulate the robust VRP-TWA to handle cases in which the probability distributions are hard to estimate. In the RVRP-TWA, it is assumed that the distributions of the travel times are uncertain and only some descriptive statistics are available. The risk of violating the assigned time windows is minimized, while ensuring that the expected travel time is lower than a certain threshold value. To measure the risk of violating the assigned time windows, the time window violation index based on the requirement violation index proposed by Jaillet, Qi, and Sim (2016) is used. An exact method is proposed to solve the subproblem of assigning a time window to each customer in a given route with a minimum time window violation index. We show that this subproblem is convex and that the subgradient cuts can be generated. These cuts are used in a branch-and-cut framework to exactly solve the RVRP-TWA. The experiments show that the branch-and-cut algorithm is able to solve instances with up to 35 customers. Furthermore, the trade-off between the expected total travel time and the time window violation index is shown. Allowing the travel time to increase by a maximum of 5% compared with the minimum travel time decreases the time window violations by, on average, 33%.

The solution quality and robustness of the RVRP-TWA model are tested by comparing it to a stochastic variant of the VRP-TWA in which the travel time distributions are known. An exact solution method is proposed for the SVRP-TWA using a branch-and-cut framework. Using the SVRP-TWA model, we have shown that the robust solution is close to the optimal solution. Furthermore, when the travel time distributions are uncertain, the robust approach performs better than the stochastic approach.

To solve larger instances, the subproblem of minimizing the time window violation index for a given routing solution could be incorporated in a heuristic framework. Furthermore, the variant of the VRP-TWA with hard time windows, in which the vehicle has to wait when it arrives before the time window, could be an interesting topic for future research. Hard time windows are more difficult to solve exactly, because the arrival time cannot be calculated by the sum of the independent travel times of the arcs. However, the stochastic variant can be solved with the sampling-based approach proposed in this chapter. It would also be interesting to develop new risk measures for the robust approach that take other characteristics of the travel time distribution into account.

8.1. Extensions: Variable Time Window Length and Correlated Travel Times

In this section, two extensions of the proposed method are discussed: time window length as a decision variable and correlated travel times.

8.1.1. Variable Time Window Length. We assumed that the length of a time window per customer is an input variable that can be chosen by the decision maker. Our approach can be extended to the case where ϵ_i is a decision variable with linear cost. The problem will become even more complex because the solution space will increase for a given route. However, the same proposed methodology and solution method can be used. Because of the extra decision variable, an extra KKT condition must be added, and therefore the subgradient will be slightly adjusted.

8.1.2. Correlated Travel Times. In practice, the travel times of arcs may be correlated. However, most papers on travel time uncertainty assume independent travel times to avoid a tremendous increase in model complexity or because of data availability. Jaillet, Qi, and Sim (2016) propose a way to include correlation without increasing the complexity of the algorithm too much. We briefly describe how this approach can be applied in our setting.

As suggested by Jaillet, Qi, and Sim (2016), the travel times can be expressed as a linear function of independent factors, that is,

$$\tilde{z}_a = z_a^0 + \sum_{j=1}^{B} z_a^j \tilde{c}_j, \quad \forall a \in \mathcal{A},$$

where $\tilde{c}_1, \ldots, \tilde{c}_B$ are independent distributed factors that represent, for example, the weather conditions, the occurrence of traffic jams, etc. The coefficients of these factors can be estimated by a linear regression. Note that this method can be used only when a lot of data are available to, first, create the distribution of these factors and, second, estimate the coeffients by regression. When the formula for $\tilde{z}_a$ is estimated, then this can be incorporated as follows:

$$\begin{aligned} C_{\alpha_i}(\tilde{t}_i) &= C_{\alpha_i}(\tilde{\mathbf{z}}\mathbf{s}^i) = C_{\alpha_i}\left(\sum_{a\in\mathcal{A}}(z_a^0 + \sum_{j=1}^{B} z_a^j \tilde{c}_j) s_a^i\right). \\ &= C_{\alpha_i}\left(\mathbf{z}^{0^T}\mathbf{s}^i + \sum_{j=1}^{B}\tilde{c}_j \mathbf{z}^{j^T}\mathbf{s}^i\right) = \mathbf{z}^0\mathbf{s}^i + \sum_{j=1}^{B} C_{\alpha_i}\left(\tilde{c}_j \mathbf{z}^{j^T}\mathbf{s}^i\right). \end{aligned}$$

When using this function in the problem formulation, the calculation of the functions $C_{\alpha_i}(\tilde{\mathbf{z}}\mathbf{s}^i)$ and $C_{\eta_i}(-\tilde{\mathbf{z}}\mathbf{s}^i)$ and their subgradients will change. The subgradients can be calculated in a relatively straightforward manner, and the proposed methodology in this paper can be applied directly.

References

Adulyasak Y, Jaillet P (2016) Models and algorithms for stochastic and robust vehicle routing with deadlines. *Transportation Sci.* 50(2):608–626.

Agatz N, Campbell A, Fleischmann M, Savelsbergh M (2011) Time slot management in attended home delivery. *Transportation Sci.* 45(3):435–449.

Agra A, Christiansen M, Figueiredo R, Hvattum LM, Poss M, Requejo C (2013) The robust vehicle routing problem with time windows. *Comput. Oper. Res.* 40(3):856–866.

Bertsimas D, Sim M (2004) The price of robustness. *Oper. Res.* 52(1):35–53.

Campbell AM, Savelsbergh M (2006) Incentive schemes for attended home delivery services. *Transportation Sci.* 40(3):327–341.

Dalmeijer K, Spliet R (2018) A branch-and-cut algorithm for the time window assignment vehicle routing problem. *Comput. Oper. Res.* 89:140–152.

Ehmke JF, Campbell AM, Urban TL (2015) Ensuring service levels in routing problems with time windows and stochastic travel times. *Eur. J. Oper. Res.* 240(2):539–550.

Ellis B (2011) Waiting for the cable guy is costing us €38 billion. *CNN Money* (November 3), https://money.cnn.com/2011/11/03/pf/cost_of_waiting/index.htm.

Gendreau M, Jabali O, Rei W (2016) 50th anniversary invited article—Future research directions in stochastic vehicle routing. *Transportation Sci.* 50(4):1163–1173.

Golden BL, Raghavan S, Wasil EA (2008) *The Vehicle Routing Problem: Latest Advances and New Challenges*, vol. 43 (Springer, New York).

Jabali O, Leus R, Van Woensel T, de Kok T (2015) Self-imposed time windows in vehicle routing problems. *OR Spectrum* 37(2):331–352.

Jaillet P, Qi J, Sim M (2016) Routing optimization under uncertainty. *Oper. Res.* 64(1):186–200.

Klein R, Neugebauer M, Ratkovitch D, Steinhardt C (2017) Differentiated time slot pricing under routing considerations in attended home delivery. *Transportation Sci.* 53(1):236–255.

Laporte G, Louveaux F, Mercure H (1992) The vehicle routing problem with stochastic travel times. *Transportation Sci.* 26(3):161–170.

Lee C, Lee K, Park S (2012) Robust vehicle routing problem with deadlines and travel time/demand uncertainty. *J. Oper. Res. Soc.* 63(9):1294–1306.

Lysgaard J, Letchford AN, Eglese RW (2004) A new branch-and-cut algorithm for the capacitated vehicle routing problem. *Math. Programming* 100(2):423–445.

Ordóñez F (2010) Robust vehicle routing. Hasenbein JJ, ed. *INFORMS TutORials in Operations Research*, (INFORMS, Catonsville, MD), 153–178.

Russell R, Urban T (2008) Vehicle routing with soft time windows and Erlang travel times. *J. Oper. Res. Soc.* 59(9):1220–1228.

Solomon MM (1987) Algorithms for the vehicle routing and scheduling problems with time window constraints. *Oper. Res.* 35(2): 254–265.

Spliet R, Gabor AF (2014) The time window assignment vehicle routing problem. *Transportation Sci.* 49(4):721–731.

Spliet R, Dabia S, Van Woensel T (2017) The time window assignment vehicle routing problem with time-dependent travel times. *Transportation Sci.* 52(2):261–276.

Subramanyam A, Gounaris CE (2017) Strategic allocation of time windows in vehicle routing problems under uncertainty. *Proc. Found. Comput.-Aided Process Oper./Chemical Process Control, Tucson, AZ*, 62.

Taş D, Dellaert N, Van Woensel T, de Kok T (2013) Vehicle routing problem with stochastic travel times including soft time windows and service costs. *Comput. Oper. Res.* 40(1):214–224.

Taş D, Dellaert N, van Woensel T, de Kok T (2014) The time-dependent vehicle routing problem with soft time windows and stochastic travel times. *Transportation Res. Part C: Emerging Tech.* 48(November):66–83.

Toth P, Vigo D (2014) *Vehicle Routing: Problems, Methods, and Applications*, 2nd ed. (Society for Industrial and Applied Mathematics, Philadelphia).

Ulmer MW, Thomas BW (2019) Enough waiting for the cable guy—Estimating arrival times for service vehicle routing. *Transportation Sci.* 53(3):897–916.

Vareias AD, Repoussis PP, Tarantilis CD (2017) Assessing customer service reliability in route planning with self-imposed time windows and stochastic travel times. *Transportation Sci.* 53(1): 256–281.

Zhang C, Nemhauser G, Sokol J, Cheon M, Papageorgiou D (2015) Robust inventory routing with flexible time window allocation. Preprint, submitted January 15, http://www.optimization-online.org/DB_HTML/2015/01/4744.html.

Zhang Y, Baldacci R, Sim M, Tang J (2019) Routing optimization with time windows under uncertainty. *Math. Programming* 175(1–2): 263–305.

Zhang Y, Zhang Z, Lim A, Sim M (2018) Robust data-driven vehicle routing with time windows. Preprint, submitted November 29, http://www.optimization-online.org/DB_HTML/2018/11/6955.html.